INVITED PAPER

Radio-Frequency Rectifier for Electromagnetic Energy Harvesting: Development Path and Future Outlook

This paper reviews the evolution and the historical milestones/breakthroughs of electromagnetic energy conversion techniques over the years with an emphasis on low-density energy-harvesting technologies.

By Simon Hemour, *Member IEEE*, and Ke Wu, *Fellow IEEE*

ABSTRACT | The roadmap evolution and historical milestones of electromagnetic energy conversion techniques and related breakthroughs over the years are reviewed and presented with particular emphasis on low-density energy-harvest technologies. Electromagnetic sources responsible for the presence of ambient radio-frequency (RF) energy are examined and discussed. The effective use and recycling of such an ambient electromagnetic energy are the most relevant and critical issue for the current and future practicability of wireless energy-harvesting devices and systems. In this paper, a set of performance criteria and development considerations, required to meet the need of applications of ambient electromagnetic energy harvesting, are also derived from the radiating source analysis. The criteria can be calculated from a simple measurement of the *I*–*V* nonlinear behavior of RF rectification devices such as diodes and transistors, as well as linear frequency behavior (*S*-parameters). The existing rectifying devices are then reviewed in light of the defined performance criteria. Finally, a technological outlook of the performances that can be expected from different device technologies is assessed and discussed. Since the proposed spindiode technology would present the most promising device platform in the development of the most useful ambient energy harvesters, a special highlight of this disruptive scheme is provided in the presentation of this work.

KEYWORDS | Ambient radio-frequency (RF) energy; backward diode; crystal rectifier; diodes; energy harvesting; magnetic tunnel junction (MTJ); metal–insulator–metal (MIM); Schottky diode; spindiode

I. INTRODUCTION

Our world has been facing a series of major and serious energy-related challenging issues because of a continued and expanded industrialization as well as a seemingly endless and sometimes egoistical material consumption of human activities. On the one hand, ever more energy is needed to sustain the development of human society in connection with better productivity [1], better economic output [2], and better health [3], [4], especially in developing countries. On the other hand, our human footprint should be shrunken as much as possible to preserve the living conditions provided by nature. Air pollution, for example, should be reduced to a possible minimum because of its responsibility for most of the energy-related health issues [5], [6].

The first power plants were built to fuel the development of our modern society at a time when the demand for electricity was geographically concentered. However, the energy production, consumption, and transportation model is very different today [7]: the demand for electricity is in an unprecedented increase for powering portable and embedded devices, which are now geographically

Manuscript received July 1, 2014; revised August 29, 2014; accepted September 6, 2014. Date of publication October 14, 2014; date of current version October 16, 2014. This work was supported in part by the Government of Canada Postdoctoral Research Fellowship program and the Natural Sciences and Engineering Research Council of Canada (NSERC).

The authors are with the Poly-Grames Research Center, École Polytechnique de Montréal, Montréal, QC H3T 1J4, Canada (e-mail: s.hemour@ieee.org; ke.wu@ieee.org).

Digital Object Identifier: 10.1109/JPROC.2014.2358691

distributed. Consequently, those large, centralized electricity generation plants and heavy transportation systems (grids) are no longer suitable for supporting the sustainable development of current and emerging generations of small, mobile, countless, and scattered devices and agents.

The true solution to this problem necessitates, among others, an effective implementation (at the location where the energy is needed) of microscaled sources that are able to harvest ambient energy. This is really a technological challenge because this type of energy is usually of low density and weak compared to our common power supply. Nevertheless, this type of source truly meets the social and technological demand for long-term and sustainable development if successfully harvestable and used. This is because it harnesses an energy that is already distributed in space, and it is basically omnipresent. In fact, harvesting the surrounding or ambient energy is the natural survival strategy of most of the living species on Earth. Most exploitable ambient energies can be found in solar radiation (electromagnetics) and physical movements (mechanics), and they are successfully being harnessed with solar panels [8] (found, for example, in some calculators) and kinetic energy harvesters [9] (found, for example, in some pendulum-watches), respectively.

Like air, water, and minerals, electromagnetics present an extremely important natural resource for human life and social development, which has been particularly in support of data delivery, parameter sensing, and energy transmission through various wired and wireless platforms. This low-power density but omnipresent electromagnetic radiation originated from various human activities can thus also be harnessed.

Regardless of energy sources, the harvester, in most cases, heavily depends on the diode, which eventually enables switching-type conversion [like direct current to direct current (dc–dc) or alternating current to direct current (ac–dc) conversion] [10]. The diode (formerly known as "crystal rectifier," or simply "rectifier") is a conceptual element supposed to react differently depending on the sign of the voltage across it.

The virtues of the diode are too present in our life to be noticed but the development of our modern society is strongly related to the evolution of the rectifier, which cannot be ignored. In total, 18 Nobel Prizes have been awarded in relation with the discovery and development of rectifier devices (diodes) and their technologies [11]–[36] The impact of those nonlinear technologies on our society is truly striking: without them, electronic signal could not be processed, and electric current would just be useful enough for powering motors, heaters, and light bulbs. Without diode effects, there are no transistors and all the digital world along with them.

The diode presents a cornerstone of green energy. It has a central role in the converter modules that are very important in the harvesting and conversion process. Diodes can be found in solar panel harvesters, wind/ocean-wave energy harvesters, thermal harvesters, kinetic energy harvesters, radio-frequency (RF) and electromagnetic energy harvesters, and so forth.

Interestingly, the current diode technologies have become the fundamental cause of limitation when one attempts to shrink the size of a harvester and/or harness a low-power energy such as ambient electromagnetic energy. As a series of applications are anticipated and emerging (low duty-cycle mobile devices, ubiquitous wireless-enabled electronics), low electrical power (less than microwatts or milliwatts) needs to be harvested and provided with efficiency and effectiveness. The fast-paced Moore's law-governed progress in complementary metal–oxide–semiconductor (CMOS) technology node and microelectronic system developments suggests that microwatts and nanowatts low-power electronics are becoming more and more vital for future wireless devices, and systems such as hugely expected fifth-generation wireless systems and beyond that will integrate together the wireless data communications and internet of omnidistributed things. Therefore, the effective harvesting and practical use of an ambient electromagnetic energy in powering those mobile and wireless devices will become a reality in a not-so-distant future. Generally speaking, the harvested RF energy may be able to provide an input power in the order of tens of microwatts or less. At this power level, RF-to-dc conversion (or rectification) is quite inefficient. But the problem does not originate from the RF harvesting circuitry, which is not affected by the power level. Instead, the core of the RF-to-dc converter, a nonlinear device, is so influenced by input power that all the RF circuits are designed according to it and its surroundings. A theoretical conversion efficiency close to 100% would be attainable if not limited by this core element.

To understand the operation of rectifier devices and their limitation as power harvesters, this paper first reviews the milestone work and technological evolution of those devices over the years. Since power sources and end-user devices (the device to be powered by harvester) also play a key role in the harvesting process, they are also addressed briefly. This paper provides a global insight into the evolution of and the relationship between diode technology, ambient RF power, and power requirement of end-user device, which highlights why RF energy harvesting has been of interest only since the beginning of this century. Typical sources of ambient RF power are identified to derive metrics necessary to assess the involved rectifier technologies. The main and unified metric is theoretically derived and concerned with the zero-bias short-circuit current responsivity. The devices are compared on the basis of this responsivity in a chronological chart of diode evolution. Toward the end of the paper, a general comparison of practical rectifier devices with consideration of their parasitic components for the case of harvesting a WiFi ambient signal is summarized and discussed.

This paper addresses various aspects of diode technologies with the perspective of ambient RF energy harvesting. Most of the analysis presented in this work also holds true for zero bias power detection where high sensitivity is required. The goal of this paper is not detailing a comprehensive history of diode research and development but rather synthesizing application requirements on the one hand and the existing diode technologies on the other hand, to bridge the fundamental gap between the electronic device/diode research and the RF power-harvesting development. The bright future of emerging diodes based on Spintronics for ambient electromagnetic energy-harvesting applications and low-power ultrarapid electronics is also pointed out.

II. OVERVIEW OF RF ENERGY HARVESTING

A. Sources Responsible for Ambient RF Energy Generation

Electromagnetic radiation-based ambient power harvesting implies that the RF energy is not created deliberately and sent on purpose, but it is rather omnipresent in the ambient because of numerous natural reasons and human activities (for example, natural radiation phenomena, wireless communication and sensing, radio and TV broadcasting). Natural electromagnetic radiation involves blackbody radiation [37], where the most powerful source even at RF is the sun for our Earth environment. As a matter of fact, the solar irradiance amounts to 1×10^{-16} ($W/cm^2 \times$ Hz) at microwave frequencies [38], which, for example, corresponds to 10 nW/cm^2 over a frequency band of 100 MHz. The natural radiation also occasionally encompasses storm electromagnetic activities. One of the first radio receivers was a lighting recorder [39].

On the other hand, white noise from sparks was harnessed to build RF generators with fair efficiency (20%–60%) once the human began to understand the potential of radiowaves [40]. Thus, only one decade after the first demonstration of wireless telegraphy through the Atlantic Ocean [41], many Poulsen arc generators of tens of kilowatts were in service for broadcasting at above 100 kHz [42]. By 1919, the Federal Telegraph Company was already fabricating a wireless system capable of broadcasting 1 MW [40] of signal power (Fig. 1). Those systems were built up on different continents by the U.S. Navy to provide a worldwide contact with the U.S. fleet.

As time went on, such extremely bulky arc generators were then replaced by more efficient and relatively smaller vacuum tubes made in different forms and technologies [43]. In the pre-World War II times, most microwave research activities were triggered by radar applications. In this context, magnetron [44] and klystron [45] were remarkably disruptive technologies at that time. Then, the invention and subsequent rapid development of extremely small, highly efficient, and solid-statelly integrated transistors driven by low voltage [46] have led to the emergence of much higher operating frequency, significantly lower cost, and widely popular broadcasting stations and mobile phone systems. In addition to the solid-state device-enabled telecommunication services, classical radar has tremendously benefited from the solid-state device technologies for its own wide-ranged developments from high-powered military systems to low-powered commercial applications.

Year after year, RF base stations have gradually mapped every possible territory to ensure a wide network coverage

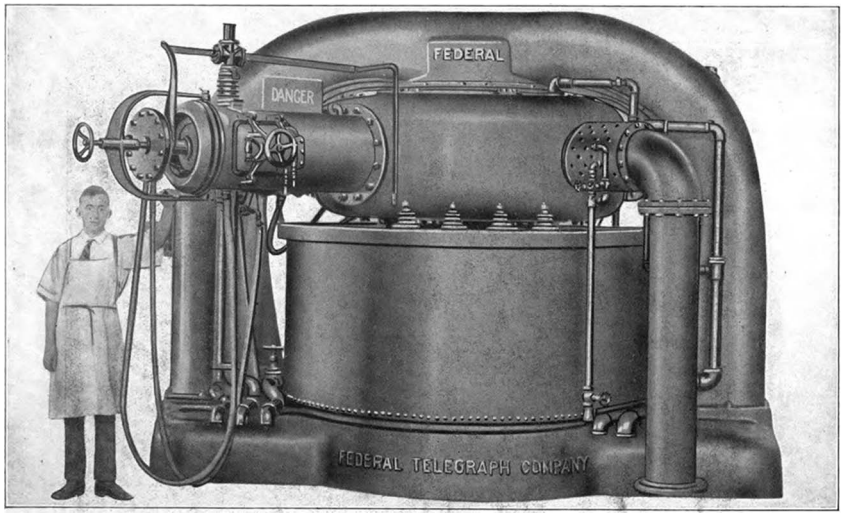

Fig. 1. *A 1-MW Poulsen arc radio transmitter in 1919. It could broadcast a continuous-wave (CW) power of 500 kW and 1 MW for a short time. (Source: Wikipedia Commons.)*

Table 1 Estimate of the Number of Worldwide Transmitter (TX) Front-Ends in Service

Million unit	Devices	Year	Ref.
12	Cell phone base stations deployed: 5.9 million of macro-cells and 6 million of small-cells (lower power, shorter range).	2012	[47]
4000	Wi-Fi enabled consumer electronics devices.	2014	[48]
6800	Subscriber identification module (SIM) cards in use.	2013	[49]

for various wireless consumers from broadcasting radio listeners to cell phone users. Some rough reported estimates of typical transceiver front–ends in service, for recent years, are summarized in Table 1. In particular, the consumer communication market is so much developed that in almost every single urban or human crowd area on the planet intended and nonintended radio-wave activities can be expected to be omnipresent.

Fig. 2 gives an example of such wireless activities in a typical ambient environment. A power density level in the order of 10 nW/cm^2 can be usually observed over certain frequency ranges for which broadcasting and wireless mobile systems have actively been deployed. Of course, such an RF power density is not always constant and uniform over space and time because of multipath electromagnetic wave propagation effects, nonuniform base-station grids, and various human-related movements. These omnipresent ambient electromagnetic sources have created an unprecedented opportunity for RF power harvesting and energy renewal or recycling. Generally speaking, narrowband signals are appropriate in connection with high-quality factor (high-Q) harvester circuits, and they are available all the time, which is highly desirable for most applications.

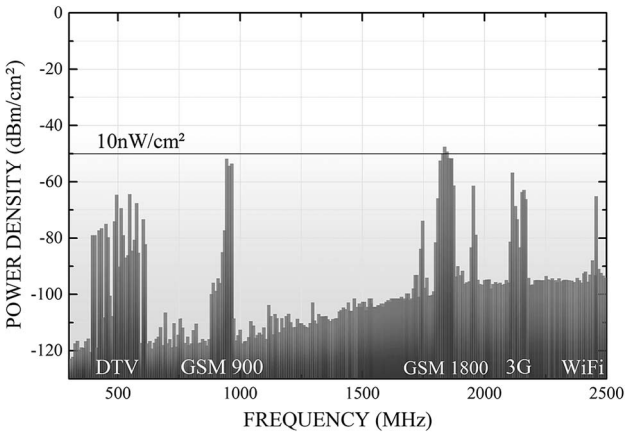

Fig. 2. *Power densities measured on a street nearby the Waterloo train station, London, U.K. The measurement method (max-hold measurements over three sweeps) is not accurate enough to provide a quantitative information, but these data are representative of what spectra can be expected in an urban environment. (Data excerpted from [50].)*

B. Power Metrics of Energy Harvesting

The utilization of a harvested energy can be made in so many different manners that it would be difficult or even impossible to present a comprehensive perspective on the power usage of every application. This is because of a variety of metrics or figures of merit on the power expenditure. In this case, we choose to rely on the metrics of Koomey [51] that are able to describe the evolution of the electrical efficiency of computer technology running at full load (Fig. 3). The adopted metrics account for not only the processing energy but also every part of the system: RAM, hard drive, to name a few of them. It can create a relatively realistic portrait regarding the evolution of digital electronic technology that is being used in our nearly every today's electronic application. The micro-Joule unit chosen here, for example, is equivalent to harvesting of −20-dBm RF power along with 10% rectification efficiency (1-μW dc power) during 1 s. In a similar fashion as the well-popularized Moore's law, the tendency seen in Fig. 3 suggests that, at a fixed computing load, the amount of a requested harvesting energy would fall by a factor of two every year and a half.

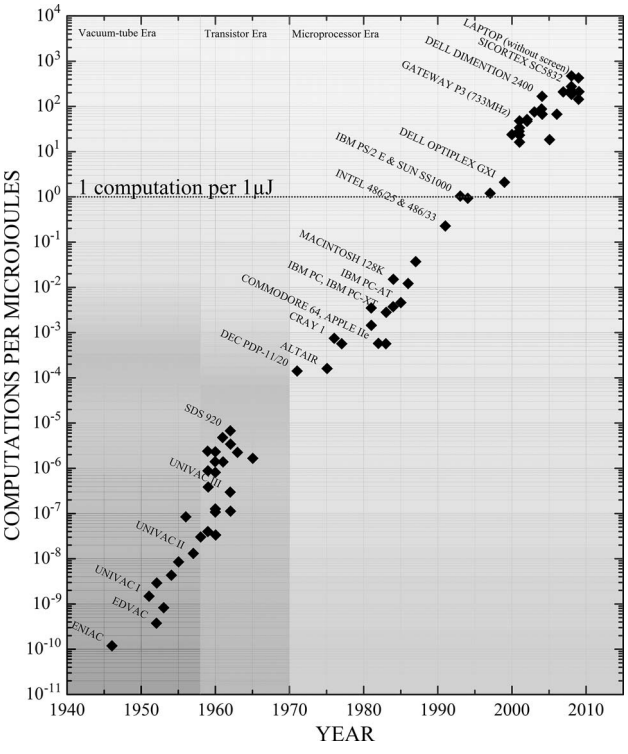

Fig. 3. *Number of computations per micro-Joules averaged over an hour. A micro-Joule is the sum of 1-μW power during 1 s, or 100 nW during 10 s. (Data from [51].)*

Interestingly, this plotted evolution inherently explains also why the field of RF energy harvesting is relatively new and emerging. As a matter of fact, the idea that the RF harvested energy is worthwhile and eventually becomes useful has been considered only for the last 15 years or since the beginning of this century. This indirectly suggests that early attempts by many researchers including the pioneered work of Tesla were deemed to fail and basically produce zero commercial interest in connection with applications at that time.

C. RF Power-Harvesting Case

With reference to the previous arguments and observations, the utilization of a harvested RF power from the ambient environment should cope with two real-life challenges: 1) low (less than 10 nW/cm^2) RF power density; and 2) limited computational capabilities.

The problem related to a low amount of RF radiated power can be alleviated by storing the harvested energy into battery cell or even in supercapacitor. Of course, this is a slow and time-sensitive process. The second issue implies that merely simple operations can reasonably be expected from the harvested power, which may perfectly concur with the power consumption profile of wireless sensors. This means that only powering low duty cycle devices is meaningful for current applications. Moreover, the size of an RF energy harvester is usually designed to be small as compared to that of other harvestable sources of energy (thermal, mechanical, etc.). It is well known that an antenna or antenna array can be enlarged and designed to coherently capture more wireless energy, which could present an approach to enhancing the received power. However, it is not appropriate as the size of the power harvester will be too large to be practical.

Fig. 3 provides a very optimistic outlook into the future where it will be expected to improve the smartness of sensors and execute the current operation with less power. Nevertheless, this projection would project light on the limitation of current power harvesters. To be specific, it becomes more and more possible to operate with less power thanks to the advancement of device technologies. Unfortunately, the harvesters would fail to harvest lower power. Fig. 4 clearly shows how current harvesters are hurdled at low power (μW). This limitation is solely caused by the inherent physical and electrical properties of rectifier devices used in the design of harvesters for the RF-to-dc power conversion. It is thus important to take a dive into rectifier technology to understand their fundamental limitations and strengths.

III. OVERVIEW OF RECTIFICATION TECHNOLOGIES

The rectifier device is a device or a circuit that converts RF-to-dc signal/power. The core conversion mechanism lies in the physics of a deployed nonlinear junction. Transistors may be used to accomplish the rectifying functions, for example, CMOS-based rectifiers. Judging from the conversion efficiency and power management, a diode is definitely the mainstream technology for the design and development of various rectifiers. To formulate a comprehensive representation of the rectifying techniques, this section will look into the historical milestones and background of rectifier development. This allows us to discuss and spell out the strength and limitation of each rectifying technology. Only the physical mechanisms for rectification existing at zero bias are considered since they are of interest to true RF and wireless power-harvesting applications. A nonzero bias rectifying operation requires external energy and is therefore not suitable for RF energy-harvesting applications.

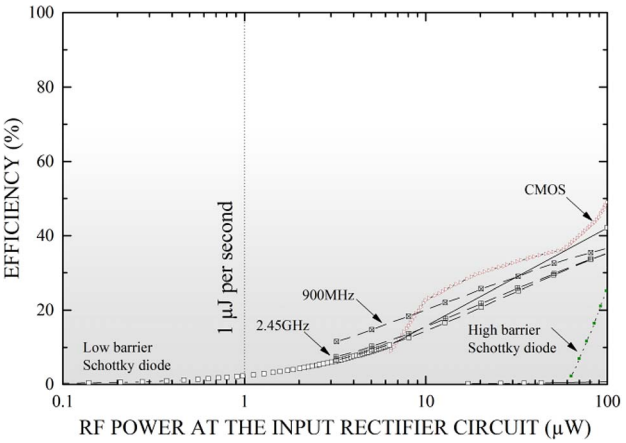

Fig. 4. *State-of-the-art microwave rectifier circuits (measurements). Color and shape of the scatters stand for which nonlinear device a circuit of interest is based on. (Figure from [52].)*

As was already understood 14 decades ago (1875), different materials brought in contact can result in a "deviation from Ohm's law" [53]. This is the physical foundation for the formation of diodes and transistors. Today, there are four fundamental diode technologies, which are competing to offer the highest deviation—namely, current–voltage nonlinearity—that is responsible for RF-to-dc power conversion. These developed technologies are presented in Fig. 5, and their enabling material combinations are indexed in Table 2. As will be demonstrated in Section IV, the most critical parameter to evaluate the rectifying capabilities of a diode technology is the short circuit current responsivity. This parameter is a direct function of the $I(V)$ characteristic curvature and is defined in (7), formulated in Section IV. Throughout this section, as well as in Fig. 5, the responsivity will be used to show and characterize the evolution of rectification over the years. Some of the points drawn in this figure are extracted from early reports of current–voltage data that were presented graphically. The extraction of current responsivity implies the second-order derivative of such a

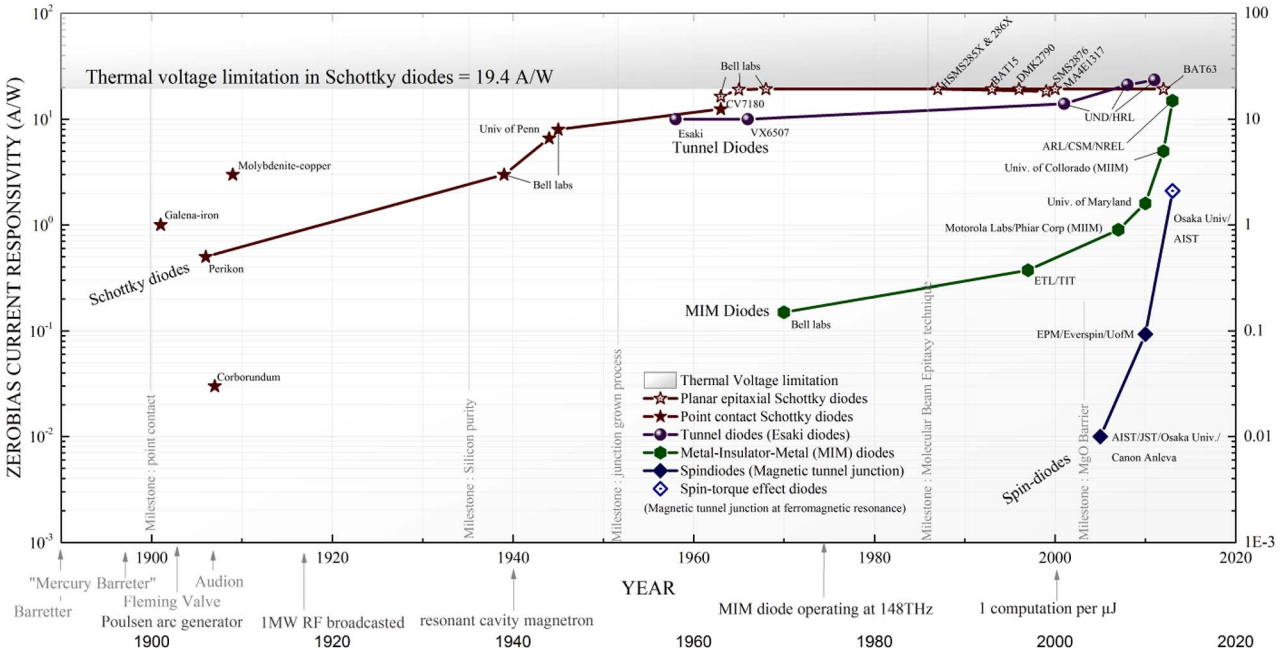

Fig. 5. ***Evolution of the rectification capabilities of different diode technologies over the years.***

curve. The discretization (then digitalization) of the $I(V)$ curves thus becomes a source of error for data accuracy. In fact, Fig. 5 is intended neither to be comprehensive nor to report a quantitative evolution of rectifiers, but rather to shed light on the trends of the progress in this connection, aside with the technological milestones that enable it.

The most efficient way to deviate from Ohm's law is to restrict the normal flow of electron using a barrier of potential. Depending on the structural topology, the electron will likely move across the barrier by a thermal activation (for example, Schottky diode) or tunnel the barrier [for example, tunnel diode, metal–insulator–metal (MIM) diode, spindiode] by a physical effect.

The "deviation from Ohm's law" was first reported in 1874–1875 by Ferdinand Braun and Arthur Schuster [53], [54]. However, it remained a pure academic curiosity for two decades. In fact, it is only after the world realized the potential of radiowaves in 1901 on the day of the first transatlantic wireless transmission [55], that the interest in RF signal detection and rectification gathered real enthusiasm that stimulated a series of great inventions in connection with diode and device technology.

Table 2 Technologies of Rectifier: Combination of Materials

	Semi-conductor		Insulator
	Schottky diode	Backward (tunnel) diode	MIM diodes
Metal (charge-based operation)	★	●	⬢
Ferromagnetic metal (Charge & spin-based operation)			MTJ, or Spindiode ◆

A. Early Non-Schottky Devices

The devices briefly described in this section can deliver neither zero-bias rectification nor RF energy harvesting. For this reason, they are not even mentioned in Fig. 5. Nevertheless, as they were part of the early development landscape of RF signal detection, they played a major role during the course of rectifier development.

The micrometer spark gap resonator was first used to detect a radiowave. Employed by Heinrich R. Hertz during his groundbreaking investigations, it had a very limited sensitivity and the received signal had to be strong enough to ionize the air between the two conducting electrodes. The spark gap was mounted in series with a loop antenna [Fig. 6(a)]. To evaluate the magnitude of a received power, Hertz was adjusting the gap distance with a fine micrometer screw [57]. Used up to tens of meters of transmission distance, this detector could not have any commercial application, but was setting the decisive milestone to experimentally confirm the validity of Maxwell's equations and stimulate the subsequent RF and electromagnetic explorations and exploitations for various applications.

Things radically changed when, in 1890, Édouard Branly observed that an electromagnetic wave could change the ability of metal filings to conduct electricity [58]. Based on this fact, he built up a device that Oliver

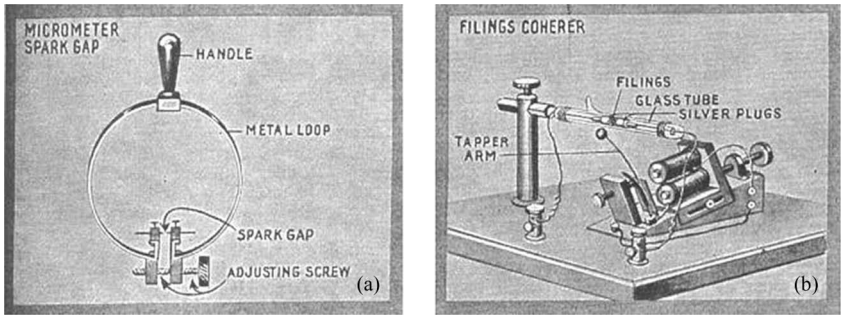

Fig. 6. *(a) Micrometer spark gap, as used at the end of the 1880s. A micrometer screw is used to vary the spark size, and thus evaluate the received power. (b) Filings coherer invented in 1890; the version seen here was used by Marconi in the first commercial radio sets. A tapper arm is used to "de-cohere" the detector [56]. (Source: http://earlyradiohistory.us/.)*

Lodge named "coherer" after its physical mechanism: In idle state, the metal filing tube had a large resistance, but when subject to a radio signal, the filing (usually a mixture of nickel and silver) would cohere, inducing a drop in resistance. The drawback of this technology was that after the filing it did not return to its initial state. In an attempt to solve the problem, Lodge added a "tapper arm" that would periodically dislodge clumped filings [Fig. 6(b)]. This detector was soon used by Guglielmo Marconi for his ship-to-shore communication system that became widely used in the first years of the 20th century. The coherer even served as a detector for the first Hülsmeyer radar in 1904 [59]. Unfortunately, the coherer could not discriminate (rectify) the magnitude of signal, and could not be used as a detector for continuous waves.

To overcome the drawback of the coherer, John Ambrose Fleming investigated the rectifying effect of the thermionic emission for the Marconi Company. Thermionic emission was first observed in 1873 by Frederick Guthrie and later rediscovered by Thomas Edison during his work on incandescent light bulb with carbon filament. Edison did not understand the phenomenon and presumed it to be a current of charged carbon particle, and then halted the investigation on this effect [60]. Fleming, who earlier worked for Edison, realized in 1903 that thanks to the thermionic emission, electrons were able to flow only in one direction. He improved the device design and performance, and patented it under the name of "oscillation valve" [61] for its rectifying capability [Fig. 7(a)]. When the filament material was heated up to a high enough temperature, some of its electrons were gaining enough kinetic energy to literally boil off the surface toward the plate. The oscillation valve had a strong impact on the radio detection/reception business, and became gradually widely accepted and used.

Lee De Forest, a competitor of Marconi Company at that time, was quite interested in the vacuum tube of Fleming, and tried to repatent it in the United States [62]. As he was concerned with a patent infringement lawsuit, he tried to modify the topology of the tube to bypass the Fleming's patent [61]. He eventually inserted a third electrode "grid" [Fig. 7(b)] into the space between the cathode and the anode which improved the device operation, and applied for a new patent in early 1907 [63]. Although De Forest did not understand well the operation of his triode (named "audion" at that time), it is probably the greatest invention of the 20th century because it is the first device that could amplify an electric signal. The triode later

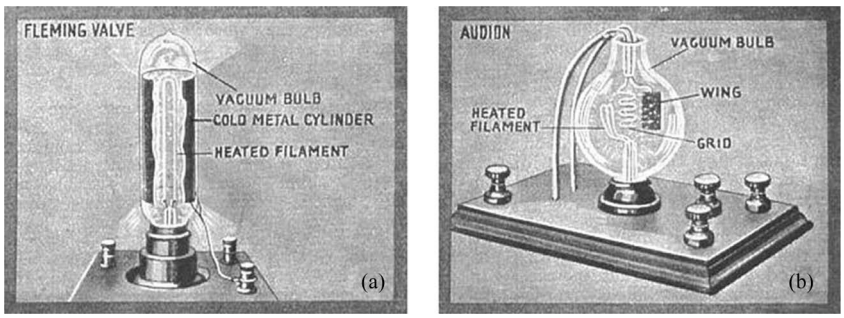

Fig. 7. *(a) Fleming valve, patented in 1904 in its commercial version [56]. Operation is based on thermionic emission of electrons from the heated filament, which were attracted only to a positively charged anode. (b) "Audion" detector (triode) invented in 1907 [56]. A grid is disposed between the filament and the plate to control the charge electron displacement. (Source: http://earlyradiohistory.us/.)*

evolved into the tetrode, the pentode, and other types of valves, thus making an efficient use of the thermionic emission. Thanks to the versatility (rectification, amplification, etc.) and high performance of the devices, the "vacuum tube era" lasted more than 50 years until the emerging of solid-state technologies. However, the constant need for a battery was making it "unhandy," if not inoperable, for many applications. Finally, because of the transit time of electrons, the device was not suitable for microwave frequencies.

1) Cat Whisker, Point-Contact Rectifiers: When the Branly's coherer started to be used commercially, nonlinear resistances, provoked by two different materials in contact, had already been reported for a while. The coherer had been exactly what was necessary to stimulate research on an RF detector: 1) sensitive enough to be used commercially as well as to show the potential applications of radiowaves to a grand public; and 2) so imperfect that significant research was necessary to find a better detector. In search for viable RF rectifier, researchers started to try-and-error different material combinations. In less than a decade, the main rectifier devices were found (Fig. 8). To achieve a good contact between two solids, they soon realized that much stain should be applied to the contact so not to leave any "gap" between materials at the atomic level. At a given force, the pressure could be increased by reducing the point contact area. Therefore, most of the designs moved toward a very thin metal wire ("cat whisker") pushed by a spring upon the crystal surface. But the contact was built from raw crystal materials, which had a nonuniform surface property. The devices were thus usually fabricated with some mechanical degree of liberty: the operator would modify (more or less by luck) the arrangement to find a suitable spot for rectification.

The quality of the interface between the materials of interest could not be controlled, and it is now impossible to tell what conduction mechanism was then responsible for the nonlinear current–voltage behavior. However, it is believed that, in most cases, the electron transport was done by a thermal activation (thermionic emission) (Fig. 9), as its height became varied upon the input RF signal magnitude.

Actually, the first metal–semiconductor contact-based rectifier did not use the cat whisker but a liquid instead. This device, the iron–mercury "autocoherer" (also called "Italian navy coherer"), has a place of choice in the textbooks of history because it was used in 1901 by Marconi for the first transatlantic communication. Although Marconi claimed its invention in 1901, it soon appeared that he had taken the work of somebody else. Paolo Castelli was rapidly acknowledged for the invention [64] [Fig. 8(a)], but it was eventually found that Jagadish Chandra Bose [65] was the first to report results on this detector in 1899.

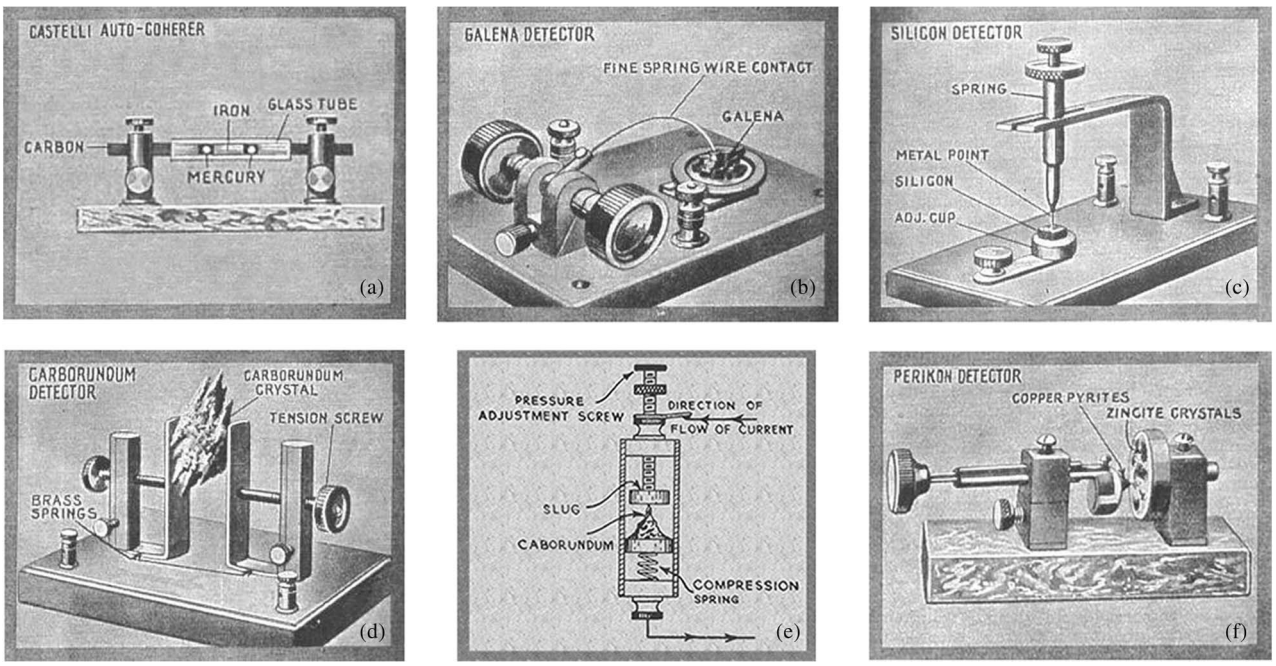

Fig. 8. *Miscellaneous contact detectors. (a) Iron–mercury autocoherer reported in 1899 by Bose and rediscovered in 1901 by Castelli. (b) Galena (lead sulfide) detector patented in 1901 by Bose. (c) Silicon detector, patented in 1906 by Pickard. (d) Carborundum (carbid of silicon) detector patented in 1906 by Dunwwody. (e) The carborundum detector was the only contact reliable enough to be packaged in a cartridge. (d) Perikon detector developed by Pickard in 1907 and used in the U.S. Navy. (Sources: http://earlyradiohistory.us/ and http://www.clarkmasts.net.au/.)*

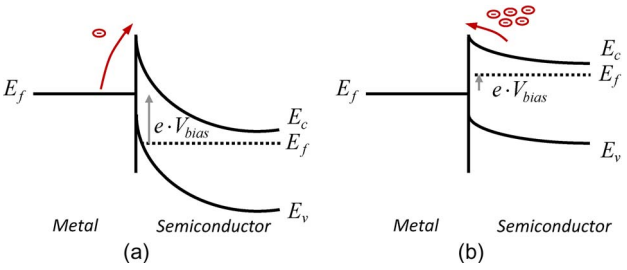

Fig. 9. *Rectification by a metal–semiconductor barrier: current is more likely to flow in case (b) than in case (a). The height of the barrier viewed from the metal is only dependent on the contact potential difference of the two materials, thus the resistance does not vary upon an external voltage. However, in (b), an external voltage will raise the electron level of the semiconductor, and the barrier height as seen from it will seem lower. The conduction current from the semiconductor to metal will then increase exponentially with the external voltage because electron energy distribution is exponential in the semiconductor, above the conduction band.*

Detecting signal was possible due to the formation of an oxide film on the interface of mercury and iron [66]. Since no current–voltage data have been found by the authors, this device is not collected in Fig. 5. The mechanical stability of the oxide layer proved to be quite unreliable, and Bose directed his researches toward Cat Whisker rectifier based on lead sulfide (Galena). This device was the first metal–semiconductor solid-state rectifier, and was patented in 1901 [Fig. 8(b)]. It was an inexpensive detector, easy to build from its early days, and became widely used, especially among amateurs. This detector was very sensitive but the contact became so unreliable that the operator had to constantly search for a "spot." Five years later, Greenleaf W. Pickard proposed to use silicon as crystal [Fig. 8(c)], for yielding better reliability. High reliability was accomplished during that same year (although at the expense of sensitivity) in 1906 when Henry H. C. Dunwwody made use of carborundum [Fig. 8(d)], a man-made material (silicon carbide) that was used at that time as a polishing abrasive. The great advantage of the carborundum material was its density. It was so hard that the cat whisker could be firmly pressed against it, thus resulting in a very repeatable point contact [67]. This detector almost did not necessitate a new arrangement of the point contact, and could be packaged [Fig. 8(e)]. The U.S. Navy was prone to the Perikon detector ("PERfect pIcKard cONtact"). In the configuration shown [Fig. 8(f)], multiple zincite crystals were provided because of their fragility. In 1909, George Pierce found that the molybdenite–copper contact [68] was very sensitive, but still not reliable. The reliability was then found in vacuum tubes, and commercial interest in crystal rectifier progressively vanished.

Responsivity of the devices is shown in Fig. 5 in a chronological perspective. Data are derived from a comprehensive comparison of $I(V)$ characteristic curves reported by Coursey [69]. The Perikon has been chosen to start the line of point-contact metal–semiconductor diodes because it had the best sensitivity–reliability tradeoff. Judging from the Schottky contact diode more globally from Fig. 5, it can be said that it started with a much higher responsivity than other technologies. The reason is that the barrier required for rectification is easily and naturally formed at a metal–semiconductor contact (Fig. 9), while a vast amount of process engineering has been necessary for the later technologies (based on electron tunneling). Rectification operation is described in Fig. 9. It is interesting to note that, at that time, many believed the nonlinearities were due to the thermoelectric effect [70], [71].

2) Semiconductor Purity and Uniformity of Doping: Three decades passed after the Fleming patent of 1903. The sensitive vacuum tube rectifier had replaced crystal schemes in most applications and engineers believed the game was over for the point contact. Interest in crystal was still omnipresent among amateurs because the vacuum tube was expensive, and handling the whisker was an experience in itself [72], but the aforementioned unreliability had basically killed any hope for commercial applications at that time.

In the 1930s, researchers began to invest efforts to harness higher frequencies. First, mobile applications were demanding smaller antenna, and second, World War II was approaching and centimeter-wave radar technology was expected to be a crucial technology for military systems. The bulky vacuum tubes, however, were not suitable for those applications. Mobility was limited due to the need of battery (high voltage), and more seriously, the transit time of electrons between the electrodes was restricting the operation frequency. Tubes were still ideal for the intermediate frequency (IF) chain of a superheterodyne receiver, but could not be used as a microwave mixer.

Scientists then turned their interest toward crystals to investigate their erratic and unreliable behaviors. Russell Ohl, who provided the most contributions during that period, thought that drawbacks of the cat whisker diode were caused by the impurities in crystal, more than crystal itself. As an electrochemist by education, he understood that crystals used in the detectors were not uniform, and that only a right kind of impurity would give the best responsivity. Thus, he first pushed for ultrapure crystal [73]. By 1939, silicon crystal ingot purity attained 99.8%. When ingots were polished prior to be contacted by the cat whisker, resulting rectifiers showed a behavior so reliable that any part of silicon wafer could be used to yield the same result. Searching for the right spot was no longer necessary and the point contact could be packaged, ready for rugged applications (Fig. 10).

As can be seen in Fig. 5, responsivity did not get improved in nearly 30 years. The Bell Laboratories diodes of 1939 were not more sensitive than molybedine–copper contacts of 1910. But as it gained in reliability, the point contact could return to commercial/military applications.

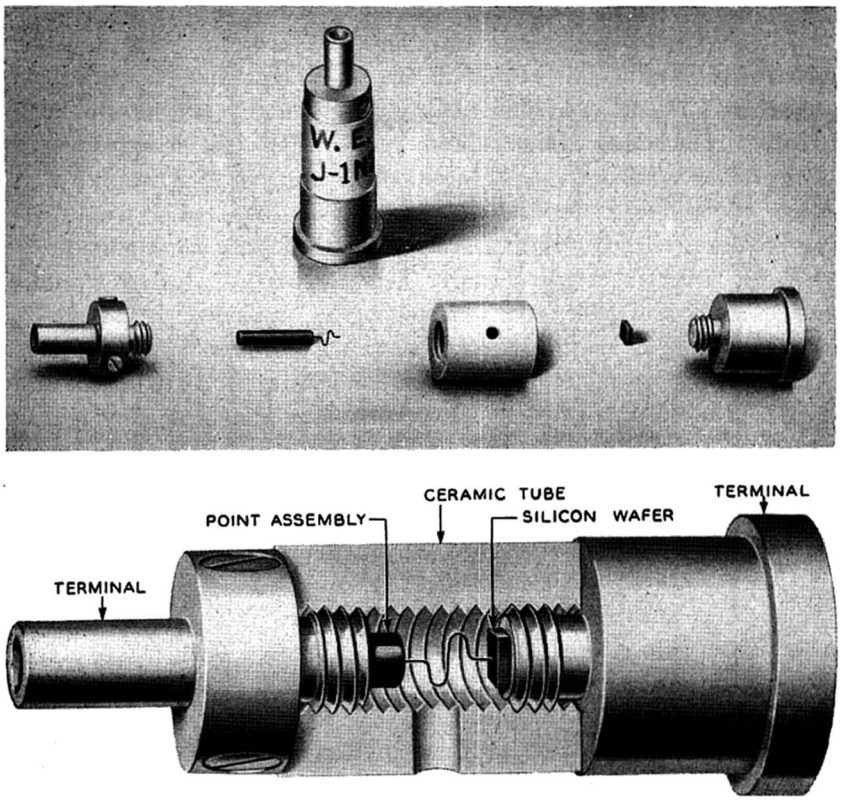

Fig. 10. *Silicon point contact diode in its 1941 form (from [75], copyright (2014) by Alcatel-Lucent). It was the first diode fabricated at a large scale and was primarily used in the Allies' radar systems during World War II.*

The diode rapidly became a key building element in the front–end mixer within radar systems, so precious in the wartime. Crystals were reliable but far from being perfect. Radar sensitivity was still poor due to a low mixer efficiency. With purity of a semiconductor being settled down, Ohl moved toward the improvement of the doping level. Extensive studies of silicon preparation and ion bombardment resulted in a better control of the doping process and its uniformity [74]. This led to a rapid improvement of the nonlinearity of the metal–semiconductor point contact. It enabled the mixer to improve its conversion losses and zero bias power detector to reach a higher responsivity. Fig. 11 shows the improvement of the receiver noise figure due to the improvement of the diode technology. This trend can be also observed in Fig. 5: it was during World War II that responsivity was improved most rapidly [75].

3) Junction-Grown Process: After World War II, research laboratories moved from early device development toward more fundamental research. Nevertheless, not much sensitivity improvement and related breakthroughs were obtained for nearly a decade. The discovery of the first transistor had generated a huge enthusiasm from which the diode fabrication had later benefited [76]. By 1951, the first grown junction transistor paved the way to the development of a junction diode. Planar epitaxial process along with existing process proved to be able to obtain a perfect and uniform interface with the right doping level [77], [78]. As an outstanding achievement, Simon M. Sze

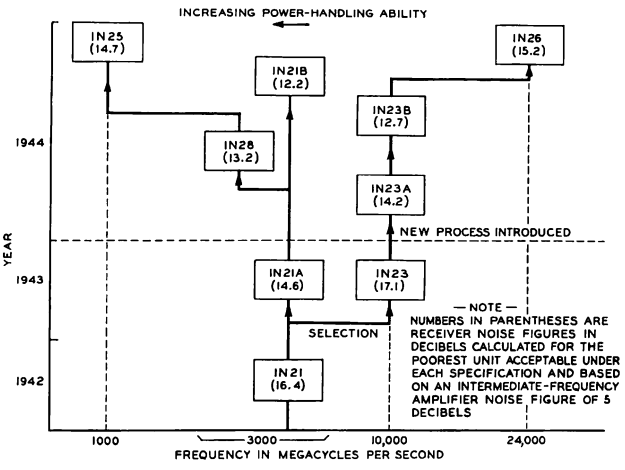

Fig. 11. *Evolution of silicon diode mixer during World War II (from [75], Copyright (2014) by Alcatel-Lucent). These were the first semiconductor diodes to be manufactured at a large scale.*

obtained a Schottky barrier diode whose forward current followed the ideal characteristics over the height order of magnitude in current [79]. The diode forward characteristic equation at zero bias in the case of "thermionic emission" carrier transport is

$$I_f = I_s e^{\frac{V}{n \times V_t}} \tag{1}$$

with I_s being the saturation current, n the coefficient of ideality, V the voltage applied to the junction, and V_t the thermal voltage

$$V_t = \frac{k_B T}{q}. \tag{2}$$

The thermal voltage depends on absolute temperature T, electrical charge of electron q, and Boltzmann constant k_B. The thermal voltage appears in the transport equation because electrons have to be thermally activated to overcome the barrier (Fig. 9).

The achievement of planar epitaxial diodes exhibited in Fig. 5 can be compared with a manufactured point-contact diode of that time, the CV7180 [80]. After that historical milestone, manufacturers worked on the process engineering to fabricate diodes with different junction resistance [81], [82], with high cutoff frequency but with the same current responsivity. Therefore, as can be seen on the chronology, it is now 50 years since the Schottky diode reached its maximum current responsivity, unable to improve further its rectifying capabilities.

Fig. 12 compares the current–voltage characteristics of a modern diode (SMS7630) with one of the early measurements of Perikon detector. The improvement of nonlinearity is clearly observed from the enhancement of forward–reverse asymmetry. It can be seen in Fig. 12(b) that the responsivity was optimized to be at its best for zero bias operation. The junction height is set to have a differential resistance low enough to be matched ($\approx$ 5 kΩ). Junction capacitance (C_j in the inset of Fig. 13) is minimized to enable operation at few gigahertz. However, note that the gigahertz operation was not new and was already possible during World War II (Fig. 11).

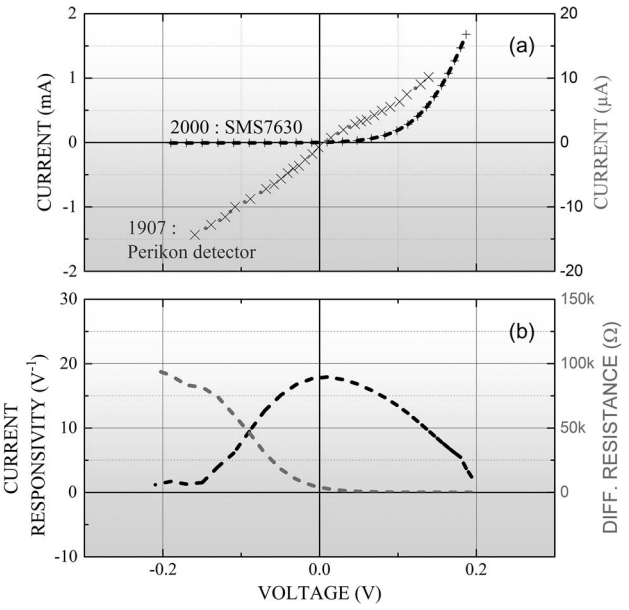

Fig. 12. *(a) Voltage–current characteristic of an early Perikon detector (1907) and a modern low barrier Schottky diode. (b) Differential resistance (right axis) of the modern device, along with the current responsivity (left axis). The device is optimized for zero bias operation.*

B. Tunnel Diodes Based on Heavily Doped Semiconductor

With the arrival of junction diode technology in the 1950s, many scientists hoped for a way to harness tunneling transport. Tunnel effect had been known theoretically for more than two decades at that time, but yet had not been observed experimentally. Interestingly, there was a general tendency in the early days of quantum mechanics that attempted to explain any unusual effects in terms of tunneling [28]. In 1956, Leo Esaki initiated the investigation of interband tunneling (also known as internal field emission) in a heavily doped p–n Ge junction [28]. If a p–n junction is adequately doped (high donor and acceptor concentration), it is possible to degenerate the two sides of the junction and place the Fermi energies within conduction or valence band. This is shown in Fig. 14(a). Thanks to this configuration, there is a probability of interband tunneling from the conduction band of the n-type region to the empty states of the valence band of the p-type region if an external voltage is applied [Fig. 14(b)].

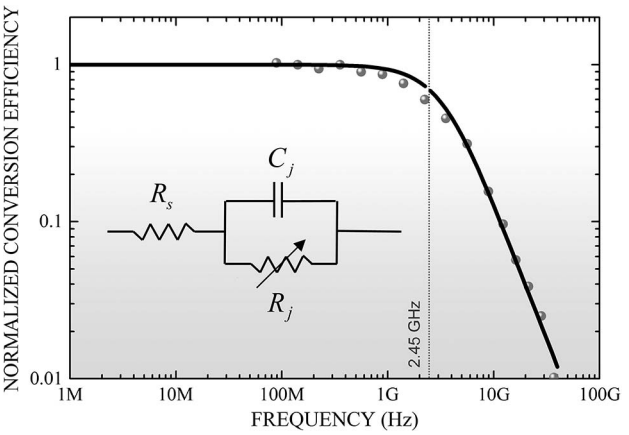

Fig. 13. *Measurement (scatters) and simulation (solid line) of the frequency-dependent RF-to-dc conversion efficiency normalized to the low-frequency value of a low barrier SMS 7630 Schottky diode.*

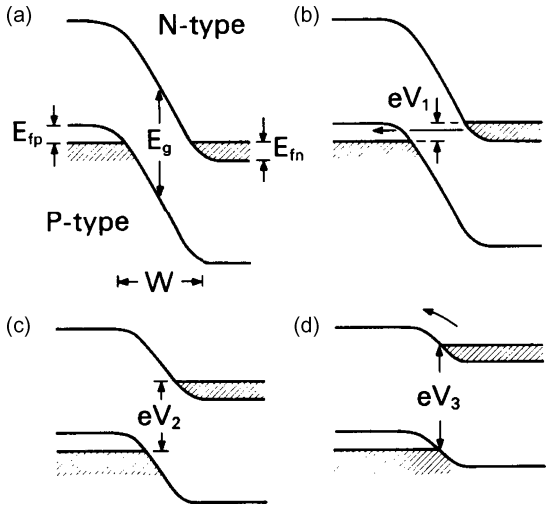

Fig. 14. *Esaki's energy diagrams at varying bias conditions in the tunnel diode [28], copyright (2014) by the American Physical Society.*

As the external voltage increases, the p-side valence band and the n-side conduction band move away from each other [Fig. 14(c)], and the current tends to decrease because of the bandgap. This continues until the thermionic emission takes over the tunneling transport [Fig. 14(d)], when electrons naturally move across the barrier under the thermal activation. From this point, the current starts again to increase as a function of the external voltage.

The transition from increase to decrease of current as a function of voltage leads the diode to a natural negative resistance phenomenon. The first paper unveiling this negative resistance was published in 1958 (Fig. 15) and yielded a massive impact, especially in the microwave community. Indeed, thanks to a low junction capacitance, the tunnel diode fitted naturally for microwave and millimeter-wave applications. Moreover, the tunnel diode was seen as a versatile device: for medium and large bias, it responded exactly like a Schottky diode, and could be used for mixer applications. Since, at the zero bias state, the diode was conducting (Fig. 16), the device had a low junction resistance, and was easy to match and very nonlinear, thus very good for power detection. Over the negative resistance region, it is possible to amplify a signal, and since the device has bias points where the junction resistance tends to be infinite, the device could be used as a switch. The fuss, however, faded with the passing years, as engineers realized that better amplifiers could be achieved using transistors, better mixers, and power detectors using Schottky diode, and better switches using low-loss p-intrinsic-n (PIN) diodes. Nevertheless, in some applications requiring excellent temperature stability, tunnel diodes exhibit superior performance than their Schottky counterparts.

Recently, interest has returned in tunnel diodes, used as "backward" diodes (a more conductive diode in the reverse direction than in the forward direction, and optimized to hold strong nonlinearities at zero bias). It came along with the necessity to develop receivers at millimeter-wave frequency, especially for imaging applications. Above 10 GHz, Schottky diodes start to be handicapped by their junction capacitance. Since the conduction is based on thermal activation, Schottky diodes are very sensitive to temperature variation, which is a serious problem in imagery.

Since the tunneling current is not thermally activated, a tunnel diode was able to break through the thermal voltage limitation (19.4 A/W at 300 K) of Schottky diode responsivity defined in (9). The Notre Dame University (Notre Dame, IN, USA) and Huge Research Laboratory (Malibu, CA, USA) team has recently made significant contributions [83], [84] with results obtained in 2011 with respect to the dramatic responsivity of 23.4 A/W [85] (Fig. 5). The band diagram of this diode is shown in Fig. 16(a). The height of the AlSb barrier is used to prevent conduction by thermal activation in the forward direction [Fig. 16(b)]. The resistance variation can be seen in Fig. 16(c). After 0.03 V, the resistance goes to infinity, which explains the increasing slope of the responsivity. Also, as predicted early [28], the zero bias responsivity is negative for a device operating with tunneling transport. The frequency behavior can be seen in Fig. 17. For a similar junction resistance, the junction capacitance of the tunnel diode is lower than that of the Schottky diode (Fig. 13). For this reason, the backward diode has better frequency performances.

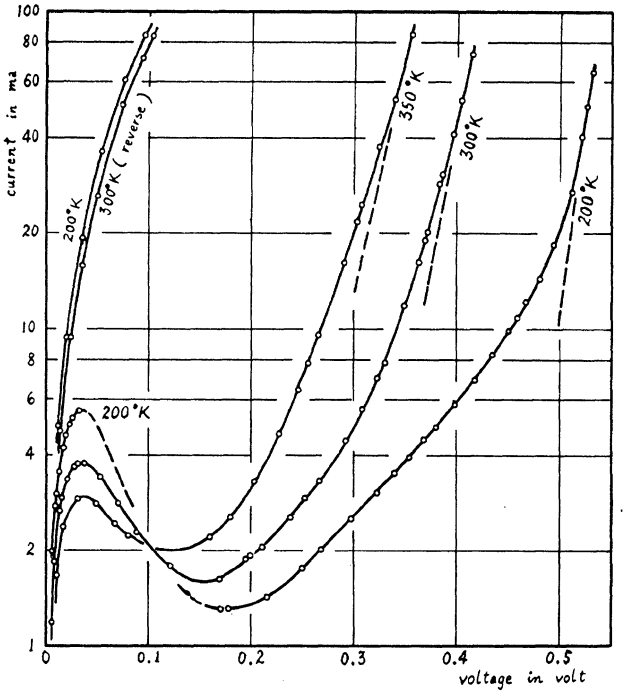

Fig. 15. *First current–voltage characteristic of the tunnel diode reported to the scientific community. (Esaki, in 1958 [86], copyright (2014) by the American Physical Society).*

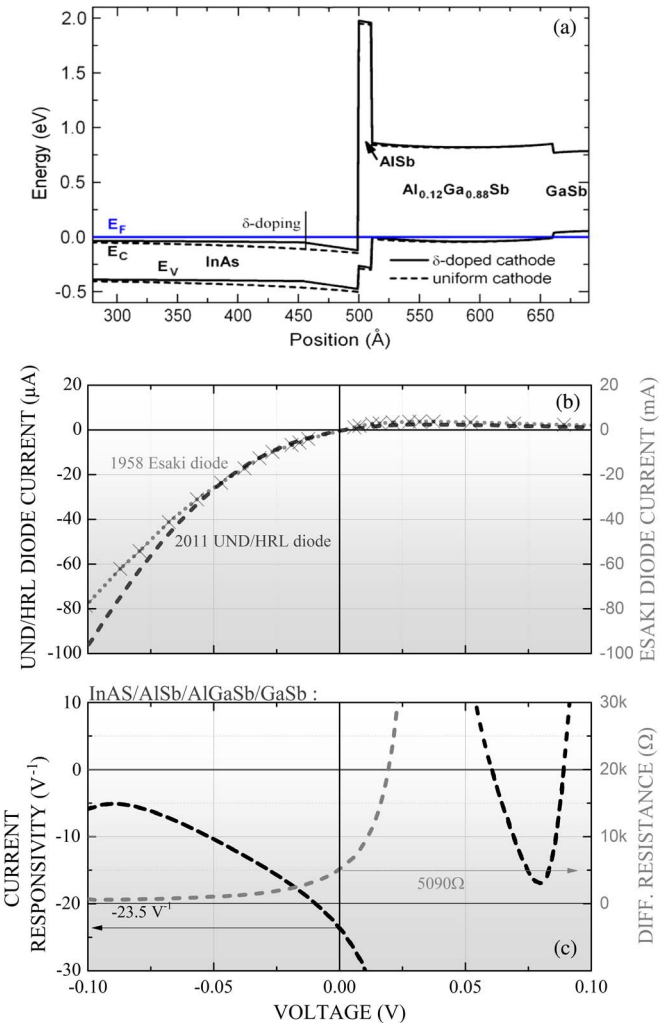

Fig. 16. *(a) Band diagram of the above-limit nonlinear tunnel diode. (b) Current–voltage characteristic of the Esaki diode compared to the 2013 UND/HRL diode. (c) Differential resistance (right axis) and current responsivity (left axis) of the later diode (inset and data from [85] and [86]).*

C. Tunnel Junction Based on MIM Structure

Back in 1927, when there were no means to prove it, a theoretical basis for tunneling transport was already proposed and established in place. First, it considered the simple case of an insulator sandwiched between two conductors [such as in Fig. 18(a)] [87], [88]. It is thus interesting to note that the first demonstration (Esaki) involved semiconductors.

In fact, an insulating barrier favorable to tunneling should be made very thin—in the order of tens of atom layers, which is extremely difficult to fabricate. By contrast, there is no need to fabricate a thin layer in the Esaki tunnel diode because the tunneling takes place through the bandgap (Fig. 14), which is naturally present in the Esaki configuration.

With the advances of fabrication and processing technology, it was becoming possible in the 1960s to build MIM junctions. Very thin insulator barrier of the order of few nanometers was achieved by a thin film deposition, which guaranteed a better control of the insulating layer over the point contact technology. It became rapidly evident that very low junction capacitance could be obtained, thus surpassing the submillimeter wave capabilities of highly doped tunnel diodes. As early as 1974, a MIM diode used as a mixer at 88 THz was reported [90], while the frequency of 148 THz was reached the following year [91].

As for Fig. 5, we chose to start the MIM timeline with the work of Brinkman [92], one of the first MIM diodes to show a significant responsivity at zero bias. The conductance–voltage characteristic of such a junction is reported in Fig. 19.

There are two transport mechanisms that mainly occur in an MIM structure, namely, the tunneling and thermal activation (thermionic emission; also called the Schottky effect). Depending on the temperature, thickness, and barrier height of the insulating layer, either mechanism predominates. If

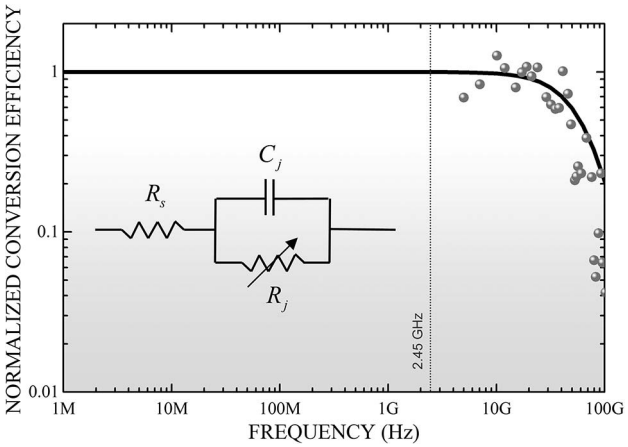

Fig. 17. *Measurement (scatters) and simulation (solid line) of the frequency-dependent RF-to-dc conversion efficiency normalized to the low-frequency value of the best backward tunnel diode reported in Fig. 5. The zero bias resistance is 5090 Ω (814 Ω.μ m^2), the zero bias junction capacitance is 2.4 fF (15 F/μm^2), and the series resistance is 103 Ω.*

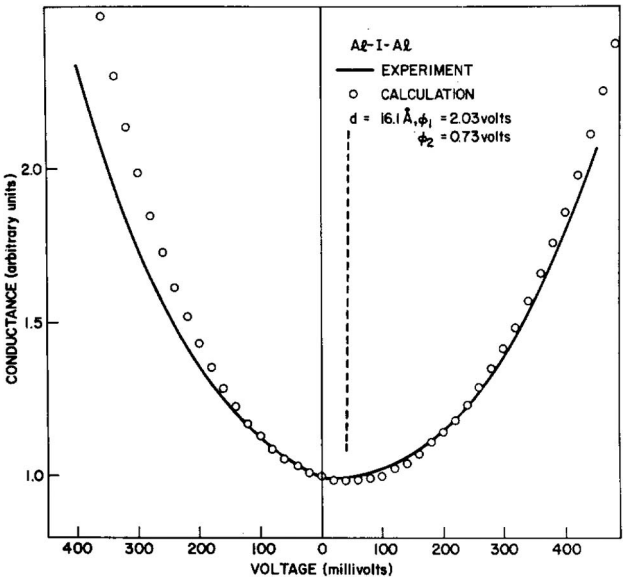

Fig. 19. *MIM diode using Al for both electrodes, as measured by Brinkman in 1970 ([92], Copyright (2014) by AIP Publishing LLC). The barrier thickness is 1.61 nm, and barrier heights on the two sides are 2.03 and 0.73 eV. The dashed line locates the zero responsivity point (ZRP). Brinkman suggested that a layer of organic impurities in the barrier oxide leads to an asymmetry of the barrier height.*

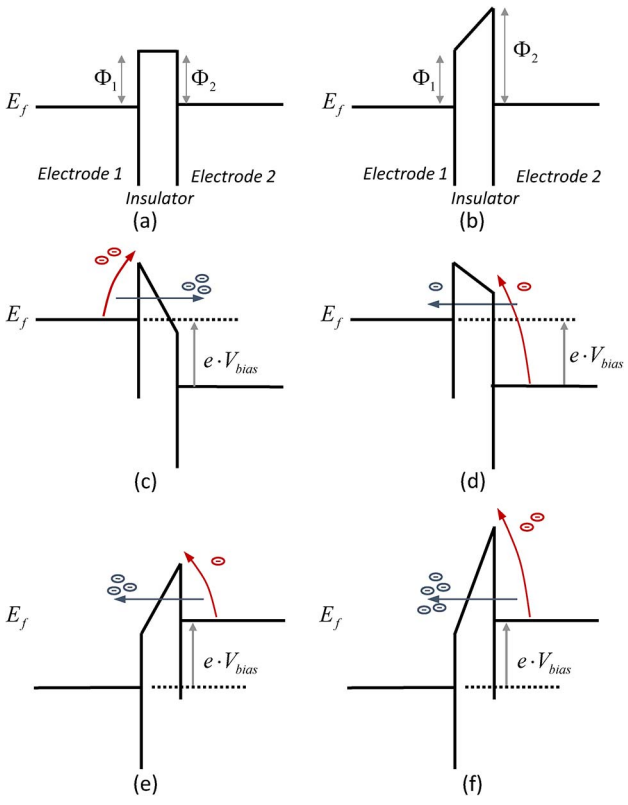

Fig. 18. *Energy diagram used by Simmons [89] in 1964 to calculate the transport properties of (a) symmetric and (b) asymmetric MIM structure. Forward bias for the (c) symmetric and (d) asymmetric case and reverse bias for the (e) symmetric and (f) asymmetric case. Blue arrows represent the tunneling transport and red arrows represent the transport by thermal activation.*

the barrier is high and thin enough, tunneling would prevail. As explained by Simmons [89], the probability of an electron to tunnel through the insulator bandgap depends exponentially on the distance it has to cover. Since this distance changes linearly as a function of the applied voltage, the current varies exponentially with the bias voltage.

It is then understandable that, in a symmetric MIM structure [such as in Fig. 18(a)], the exponential variation will be identical for both bias polarities, resulting in a minimum conductance at zero bias. Since the responsivity varies as a function of the derivative of the conductance, the responsivity at $V = 0$ is null. In an asymmetric MIM, the barrier is trapezoidal [such as in Fig. 18(b)]. Therefore, the tunneling is favored in one direction, which results in an asymmetry of the conductance. In the case of Fig. 19, the zero responsivity point (ZRP) is offset at about 30 mV.

As can be seen in Fig. 5, major improvements of MIM diode have appeared during the last 15 years. In fact, many works have been carried out to find out a right combination of materials, as well as to refine the quality of the insulating layer. For the former task, the methodology presents some similarities with the investigations of the early 1900s on cat whisker diodes. As for the later task, it consists in growing (with reproducibility) pinhole-free uniform insulating layer and high-quality metal interface. Those two tasks were tedious but the work of the early years finally paid off. That is why the MIM responsivity increased quasi-exponentially over the past years (Fig. 5). Among the MIM technology milestones, those reported in

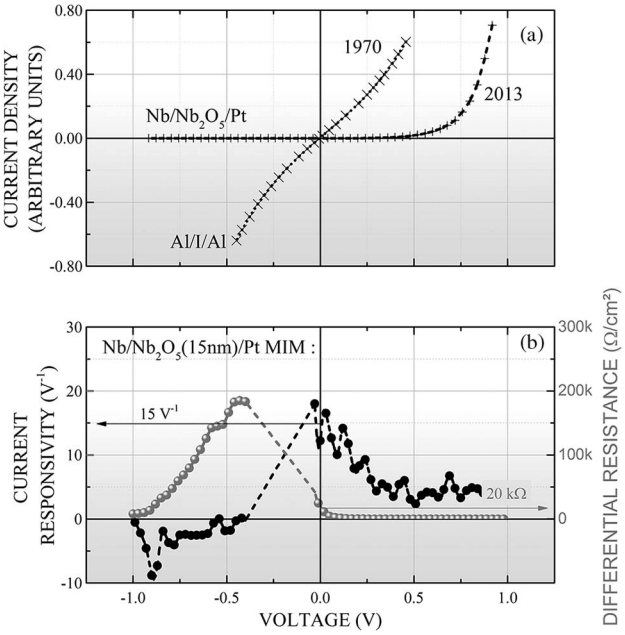

Fig. 20. *(a) Current–voltage characteristic of the stat-of-the-art Nb/Nb_2O_5/Pt MIM diode compared to the early Al/I/Al MIM structure. (b) Differential resistance (right axis) and current responsivity (left axis) of the Nb/Nb_2O_5/Pt MIM diode. (Data from [92] and [97].)*

Fig. 5 are as follows: 1) 1997—the use of a key material nobium as a first metal layer and nobium native oxide as an insulator by the joint team of the Electro-technical Laboratory (Ibaraki, Japan) and the Tokyo Institute of Technology (Tokyo, Japan) [93]; 2) 2007—the use of a double insulator structure (MIIM) by Phiar Corp. (Boulder, CO, USA) to manufacture the P1424 diode, which has been measured at 60 GHz by Motorola Labs (Tempe, AZ, USA) [94]; 3) 2010—the use of an asymmetric diode geometry (physical layout) by the University of Maryland (College Park, MD, USA) [95]; and 4) 2012—the use of a resonating double insulator barrier structure (MIIM) by the University of Colorado (Boulder, CO, USA) [96].

The highest zero bias responsivity (reported in 2013) was achieved using a Nb/Nb_2O_5/Pt structure, in a joint collaboration between the U.S. Army Research Laboratory (Adelphi, MD, USA), the Colorado School of Mines (Golden, CO, USA), and the National Renewable Energy Laboratory, (Golden, CO, USA) [97]. The later diode characteristics are reported in Fig. 20(a), and its $I(V)$ curve is compared to the curve measured by Brinkman *et al.* [92] in 1970, in order to show a large progress in nonlinearity. Fig. 20(b) shows the current responsivity, which is about 15 A/W at zero bias. The differential resistance is similar to that of a high barrier Schottky diode, whose high zero bias resistance (20 kΩ/cm^2) may not be appropriate for an RF energy-harvesting circuit.

In [97], the characteristics of the MIM diode were judiciously measured at two different temperatures for two barrier thicknesses in order to sort out tunneling effect and thermionic emission in the devices. Those results are worth a good discussion in this review because they help understand the transport mechanism and hence the rectification: measuring a diode device at low temperature is of great interest because it reduces the thermal activation so much that the quantum tunneling transport dominates. The distinction between the two modes of transport can also be made from the measurement of different barrier thicknesses as a thicker barrier would limit the tunneling possibilities.

The tunneling transport dominates in the low-temperature measurement in Fig. 21(a). It is very instructive to see that the current–voltage characteristics are quite symmetric. At high temperature, since the contribution of thermionic emission becomes significant, it can be seen that the asymmetry is more pronounced. As stated by Brinkman, the difference in barrier height is used by both transports, but in this case, it is connected to a greater effect by thermal activation. When the barrier thickness is increased, as is the case in Fig. 21(b) (15 nm), the reverse current is heavily restrained, which further enhances the zero bias responsivity. For this same diode, however, it can be seen in the low-temperature measurement that the barrier is so thick that tunneling is extinguished. As a conclusion, to obtain this best zero bias responsivity MIM device, thermionic emission necessary for the asymmetry has been enhanced at the expense of the tunneling transport.

The MIM structures are promising because they can be easily integrated with CMOS technologies. The zero bias responsivity is now close to that of Schottky diodes (Fig. 5)

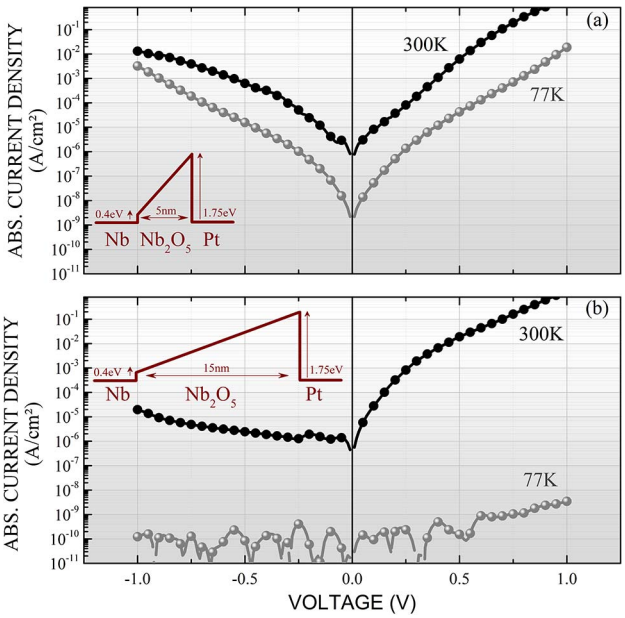

Fig. 21. *Current density versus voltage characteristics of two 80-μm × 80-μm MIM diodes having (a) 5-nm and (b) 15-nm insulator thickness (also shown in Fig. 20), measured at 77 and 300 K. Insets are the trapezoidal representation of the barrier. Data from [97].*

although more investigations are necessary to lower the zero bias resistance. Multiple insulator structures are also being investigated as they could reach similar zero bias responsivity with tunneling as the predominant transport. Those investigations are important because an MIM diode relying too strongly on thermionic emission to achieve asymmetry might exhibit a zero bias responsivity capped by a thermal voltage such as a Schottky diode. Finally, Torrey *et al.* [71] proposed that MIM rectifiers might also be built with much smaller spreading resistances than metal–semiconductor rectifiers have, which could be of great interest at frequencies where parasitic components usually degrade the performances.

Neither parameter extractions nor high-frequency measurements have been done for the diode presented in [97]. Therefore, meaningful frequency-dependent RF-to-dc conversion efficiency cannot be proposed and discussed in this section.

D. Magnetic Tunnel Junction

1) Nonresonant Rectification: Electrons have a charge and a spin whereas the carrier transport of the aforementioned three different device types and subsequently their rectification mechanisms are solely based on the charge. Mott suggested in 1936 [98] that the spin could influence the mobility of electrons in ferromagnetic material, thereby paving the way for the spin-dependent transport, as well as for the development of a new field now called Spintronics.

This field makes use of the density of states of ferromagnetic metals (see Fig. 22) that, unlike normal metals, have an imbalance of the spin population at the Fermi level (which carry the electrical current). As a result, the spin-up electrons and spin-down electrons are in different states and exhibit different conduction properties. Since it allows conduction in mostly one spin orientation (the other being scattered), the ferromagnetic metal acts as a "polarizer" and is able to lead to a spin-polarized current.

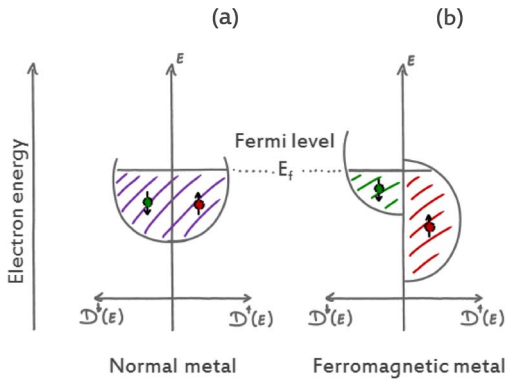

Fig. 22. *Simplified representation of the density of electronic states $D(E)$ that are available for the electrons in (a) a usual metal and (b) a ferromagnetic metal. In the latter case, the "spin-up" states are more filled than the "spin-down" states and conduction is done mainly by spin-down electrons.*

By adding a second polarizer after the first one, it is possible to create a "spin valve," where the conductance of the valve will depend on the magnetic orientation of the two ferromagnetic layers. As demonstrated by Fert *et al.* [35], [99], the ferromagnetic layers should be separated from each other by a thin nonmagnetic metal or insulator. In the latter case, the device becomes a magnetic tunnel junction (MTJ), as electrons have to tunnel (the tunneling process conserves the spin) the insulator to reach the second ferromagnetic layer (Fig. 23).

It is with an MTJ that Jullière was able to observe the first evidence of a spin-dependent transport, four decades after the Mott predictions [100]. For this, Jullière measured the ratio of resistance of the junction in parallel and antiparallel states. If spin flip (spin changing direction) is neglected during the transport, the MTJ can be seen as two independent channels: one for spin-up and the other for spin-down.

The tunnel transport can be simply described as follows: for the parallel case (the *P* state) of Fig. 23(a), in the "spin-down channel" the electron tunnels easily because the density of the state at the Fermi level is large in both electrodes (the probability of tunneling is proportional to the product of the density of states). As a result, the channel exhibits a low resistance. In contrast, as for the "spin-up channel," the spin-up states are almost completely filled, meaning that electrons will have a low tunneling probability, thus leading to a high resistance channel. Since the two channels are connected in parallel, the equivalent resistance of the MTJ is rather low in the *P* state [Fig. 23(a)].

In the antiparallel case of Fig. 23(b), spin-up and spin-down electrons in each channel will have difficulty to find free states to tunnel. As a result, less electrons can globally tunnel the structure, and the *AP* state resistance is higher. This is mostly valid for zero bias because a spin mixing due to spin-flip scattering tends to reduce the spin current polarization as the tunneling current increases under external bias. The spin mixing comes also from electron–magnon scattering, which is temperature dependent. The resulting AP state resistance behavior is of a high zero bias resistance that rapidly decreases and becomes close to that of the *P* state classical tunnel behavior. This phenomenon is extremely interesting for rectification applications because the tunneling effect and the spin mixing sums up to create more nonlinearities. At zero bias, the difference of resistance between the parallel and antiparallel states is characterized by the tunnel magnetoresistance (TMR).

A spin-dependent tunneling structure is very challenging to fabricate because any structural defect in the multilayer will provoke spin-independent scattering that will cancel the spin-dependent scattering inside the ferromagnetic layers. In this condition, the first reliable MTJ at ambient temperature was reported only in 1995 [102] using amorphous alumina as an insulating layer. But the decisive and breakthrough technological step was appended in 2004

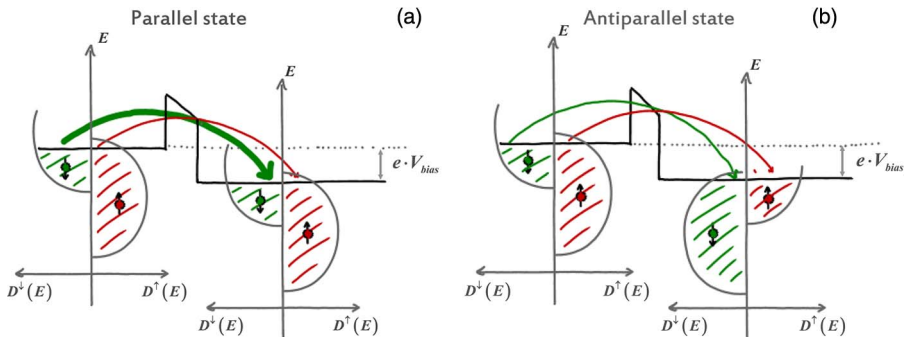

Fig. 23. *Tunnel transport in MTJ in (a) parallel and (b) antiparallel state. In the P state, the good band matching produces a high flow of electrons and a low resistance, but in the AP state, the poor band matching induces a higher resistance.*

when single crystal MTJ with MgO barrier started to get fabricated with high room temperature TMR [103]. Very high structural quality was attainable with MgO barrier, and it marked the beginning of a modern MTJ era. MTJ was integrated few years afterwards in hard disk drive, which hugely gained in both capacity and density and was eventually able to reach terabytes of capacity. MTJ is also used as magnetic random access memory (MRAM). It is expected that this nonvolatile memory technology will eventually become universal and be integrated in most of the computer architecture [104].

The first significant spindiode responsivity is indicated on the diode evolution graph (as illustrated in Fig. 5). It was reported in 2005 by a joint team of the National Institute of Advanced Industrial Science and Technology (AIST) of Tsukuba (Tsukuba, Japan), the Japan Science and Technology Agency (JST; Kawaguchi, Japan), the Osaka University (Osaka, Japan), and Canon ANELVA Corporation (Tokyo, Japan). It makes use of a MgO barrier of 0.85 nm [105] and exhibits a responsivity of 0.01 A/W at zero bias, although the authors did not mention this application.

In a study of 2012, it was proposed that the natural nonlinearity of current–voltage characteristics could be harnessed for rectification. This study conducted by a joint team of the Ecole Polytechnique de Montreal (Montreal, QC, Canada), Everspin Technologies (Chandler, AZ, USA), and the University of Manitoba (Winnipeg, MB, Canada) reported a zero bias responsivity of 0.08 A/W. It should be mentioned that the MTJ samples of this work were not designed for rectification but were only optimized for use in the development of MRAM memory [52], [101]. Characteristics of an Everspin device are reported in Fig. 24. The zero bias responsivity is not sufficient for electromagnetic power harvesting, but none of those devices have been yet optimized to maximize the zero bias nonlinearities, so it is difficult to evaluate what value can be expected. The $R(V)$ can be seen as still very symmetric [Fig. 24(b)], suggesting that there is a room for improvements. Also, the spin-dependent transport brings one more degree of freedom in the rectification mechanisms: the nonlinearities are achieved by tunneling and spin mixing. *A priori*, there is hence no reason for the responsivity to be limited by the thermal voltage.

The equivalent circuit is shown in Fig. 25. According to [52], it is derived from the small signal circuit model of a classical diode with few specificities related to the presence of ferromagnetic metal: junction inductance L_j, interfacial capacitance C_i, and interfacial resistance R_i. The effects of the junction inductance appear above 100 GHz, and can thus be neglected in the case of an RF energy harvesting. At gigahertz frequencies, the interfacial capacitance is the main limiting element, with the same low-pass effect seen

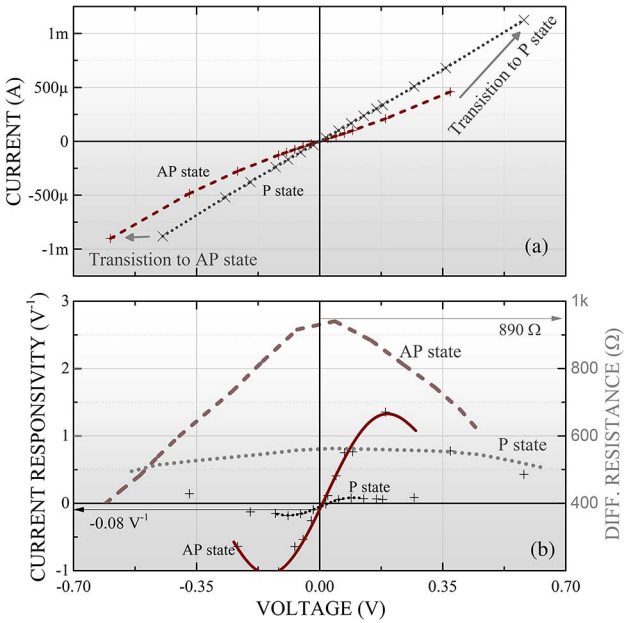

Fig. 24. *(a) Current–voltage characteristics in the P state (dot) and AP state (dash) of an MTJ (or spindiode). (b) Differential resistance (in gray) and current responsivity (in black). Responsivity measurement is shown with scatters, whereas cubic interpolation is shown with solid and dotted black line. The zero bias responsivity in the AP state is 0.08 A/W. Data from [52] and [101].*

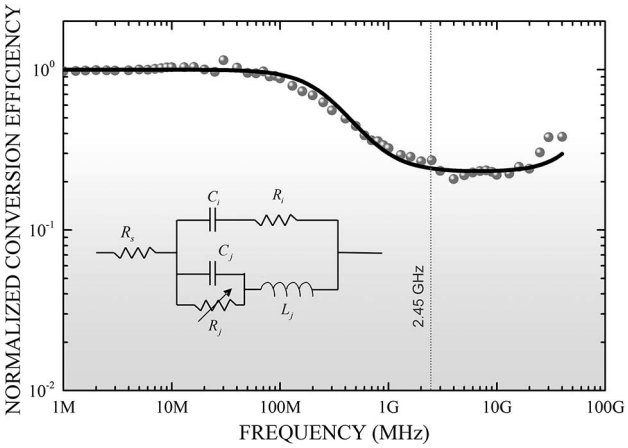

Fig. 25. *Measurement (scatters) and simulation (solid line) of the frequency-dependent RF-to-dc conversion efficiency normalized to the low-frequency value of the spindiode described in Fig. 24 and reported in Fig. 5. The interfacial capacitance is 0.88 pF, the interfacial resistance is 272 Ω, the junction inductance is 0.275 nH, the series resistance is 1 Ω, the junction capacitance is 10 fF, and the junction resistance is 890 Ω (data from [52]).*

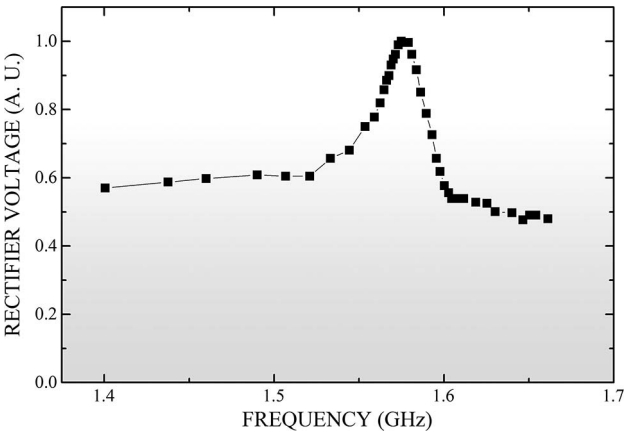

Fig. 26. *Frequency-dependent response of the spin-torque diode effect (data from [108]).*

on other diodes because of junction capacitance. C_i and R_i are used to model the spin-dependent screening effect at the interface of ferromagnet/insulator [106], [107]. In fact, much attention is usually directed to the interfacial resistance, as is quite uncommon for a diode to have a parasitic capacitance in series with a resistance. It accounts for the spin-dependent voltage drop at the interface, and has a very useful impact on the frequency behavior. In the equivalent circuit of a classical diode, the impedance of parasitic branch (Cj) drops toward zero as frequency increases. When the impedance of the parasitic branch becomes low as compared to the impedance of the junction, the RF current does not pass through the junction anymore, and cannot be rectified. In a spindiode, the impedance of parasitic branch (Ci and Ri) drops toward R_i, which, as an effect, stops the declining of performance, as can be seen in Fig. 25. It is not clear how the fabrication process impacts the interfacial resistance but, if the value could be engineered to be higher than the junction resistance, the parasitic effect would be erased below 100 GHz.

2) Spin-Torque Diode Effect: There is another thrilling effect in MTJ: it was found 20 years ago that a spin-polarized current ("polarized" by the first layer) could induce a magnetic excitation in the second layer, and even reverse its magnetization. Therefore, the RF current can impact the magnetization of the second layer, which causes a change of resistance in time. When the RF corresponds to the natural frequency of the MTJ, the RF current makes the spin valve resistance changing synchronously with the RF signal, which provokes a stronger resistance change (from the *AP* state resistance to the *P* state resistance in one RF period). A very recent publication of Osaka University (Osaka, Japan) and the Institute of Advanced Industrial Science and Technology (Tsukuba, Japan) has reported a very high "spin-torque effect" [108] of 2.1 A/W at nearly 1.6 GHz, under zero current bias condition, which has been placed in Fig. 5. It should be noted that the spin-torque effect is largely frequency dependent (Fig. 26). Therefore, it might not be suitable for broadband RF energy harvesting, but perfectly fit with narrow matching conditions often seen in the design of basic RF energy harvesters.

IV. METRICS FOR RECTIFICATION DEVICE

The device's variation of resistance as a function of input signal (ideally 0 Ω in one polarity and $+\infty$ for the other polarity) is known to be the key factor toward an effective RF-to-dc energy conversion. The most common method to evaluate rectification was used in the early development of rectennas at Ratheon (Waltham, MA, USA) [109] and later improved at Texas A&M University (College Station, TX, USA) [110] and at Shanghai Jiao Tong University (Shanghai, China) [111]. It has been also used recently for the harmonically terminated rectifier design at the University of Colorado [112]. It is employed when the variation of junction resistance is so high that the diode can be considered as a switch. This approach holds for high input power only, ideally when the input voltage is in the order of the breakdown voltage of the diode. However, for a low input power, which is the case in ambient electromagnetic energy-harvesting operation, the rectification is better described with the nonlinearity analysis, which is a formalism similar to the one used to analyze the detection process in a diode. Those methods are quite old and were nicely redeveloped in [113] and [114]. They were adapted in [52] for RF-to-dc power conversion. Some details of this analysis are reported here to provide a comprehensive understanding of the mechanism.

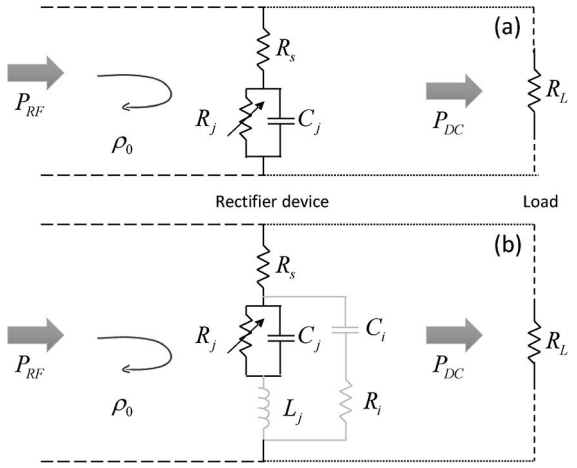

Fig. 27. *Simplified rectifier circuit for (a) conventional rectifiers (Schottky, tunnel, MIM) and for (b) spintronics rectifier. In this idealized circuit, the RF current to be rectified passes only through the dashed part of the circuit, while the dc uses the dotted path.*

Throughout this section, the idealized general circuit of Fig. 27 will be considered.

The analysis begins with the conversion itself, which appends in R_j, the nonlinear junction resistance. The current voltage characteristics are expanded in power series about the bias voltage operating point V_b. To simplify the notation, i and v are the current flowing through and the voltage across the junction resistance

$$i(v) = i(V_b) + i^{(1)}(V_b)(v - V_b) + i^{(2)}(V_b)\frac{(v - V_b)^2}{2} + i^{(3)}(V_b)\frac{(v - V_b)^3}{6} + \dots \quad (3)$$

Since the low-power harvester should not be dependent on an external dc source, there is no external bias voltage. But as the diode will rectify the RF power, the rectified voltage will change the operating point (self-bias). $i^{(1)}, i^{(2)}, i^{(3)}, \dots$ are derivatives of $i(v)$ with respect to v. If an external voltage $v_{\omega_0}(t) = A\cos(\omega_0 t)$ of magnitude A and pulsation ω_0 is applied across the junction resistance, v can be substituted by v_{ω_0} in the junction current (3), which results in

$$\begin{aligned} i(V_b,t) = {} & i(V_b) \\ & + \left[\frac{A^2}{4}i^{(2)}(V_b) + \frac{A^4}{64}i^{(4)}(V_b) + \dots\right] \\ & + \left[Ai^{(1)}(V_b) + \frac{A^3}{8}i^{(3)}(V_b) + \dots\right]\cos(\omega_0 t) \\ & + \left[\frac{A^2}{4}i^{(2)}(V_b) + \frac{A^4}{48}i^{(4)}(V_b) + \dots\right]\cos(2\omega_0 t) \\ & + \left[\frac{A^3}{24}i^{(3)}(V_b) + \frac{A^5}{384}i^{(5)}(V_b) + \dots\right]\cos(3\omega_0 t) \\ & + \dots \end{aligned} \quad (4)$$

As can be seen, the nonlinearities of the junction resistance spread the RF power through the harmonics. In this analysis, it will be considered that the rectifier is harmonically terminated [112] and that no power is dissipated in the harmonics $k\omega_0$, with $k \geq 2$ a positive integer. The RF power at the pulsation ω_0 that is absorbed by junction resistance $P_{R_j}|_{\omega=\omega_0}$ is calculated as the averaged product of the RF voltage v_{ω_0} and RF current i_{ω_0} (which is in (4), third line):

$$P_{R_j}|_{\omega=\omega_0} = \frac{1}{T}\int_0^T v_{\omega_0}(t)i_{\omega_0}(t)\,dt$$
$$P_{R_j}|_{\omega=\omega_0} = \frac{A^2}{2}i^{(1)}(V_b) + \frac{A^4}{16}i^{(3)}(V_b) + \dots \quad (5)$$

where T is the period of the continuous-wave (CW) input RF signal. The rectifying capabilities of a device are usually quantified with the current responsivity $\Re_I$

$$\Re_I = \frac{i_{sc}|_{\omega=0}}{P_{R_j}|_{\omega=\omega_0}} = \Re_{I_0}\Delta \quad (6)$$

where $i_{sc}|_{\omega=0}$ is the dc short circuit current [the term in the second line in (4)] resulting from the rectification. When a nonlinear device is driven with a low input power, the rectified current varies linearly to the RF power. In this case (square law regime), the current responsivity is constant and equal to the quadratic responsivity $\Re_{I_0}$. The quantity Δ accounts for the deviation from the linear detection. The advantage of the quadratic current responsivity $\Re_{I_0}$ is that it can be predicted from the current–voltage characteristics, by substituting $P_{R_j}|_{\omega=\omega_0}$ through (5)

$$\Re_{I_0}(V_{\text{bias}}) = \frac{1}{2}\times\frac{i^{(2)}(V_{\text{bias}})}{i^{(1)}(V_{\text{bias}})} \quad (7)$$

consequently

$$\Delta = \left[\frac{1 + \frac{A^2}{16}\times\frac{i^{(4)}(V_b)}{i^{(2)}(V_b)} + \dots}{1 + \frac{A^2}{8}\times\frac{i^{(3)}(V_b)}{i^{(1)}(V_b)} + \dots}\right]. \quad (8)$$

The low-level current responsivity $\Re_{I_0}$ sometimes referred to as β_0 is commonly used by a manufacturer to describe the diode detection performances. In the case of the Schottky diode, assuming a perfect coefficient of

ideality ($n = 1$), the low-level current responsivity is limited by the thermal voltage defined in (2)

$$\Re_{I_0} = \frac{q}{k_B T} = \frac{1}{V_t}. \tag{9}$$

In the following, it will be considered that $\Delta = 1$ for more clarity. The approximation is valid since the harvested power level is usually low. For a higher level, one would just have to consider the real value of Δ. The current $i_{sc}|_{\omega=0}$ can be converted to a Thévenin equivalent voltage source

$$V_{th} = i_{sc}|_{\omega=0} R_j = \Re_I R_j P_{R_j}|_{\omega=\omega_0} \tag{10}$$

with R_j the junction resistance. Then, the dc flowing in the load R_L (the dotted part in Fig. 27) is

$$i|_{\omega=0} = \frac{\Re_I R_j P_{R_j}|_{\omega=\omega_0}}{R_j + R_s + R_L} \tag{11}$$

with R_s the series resistance of the diode.

The total dc power $P|_{\omega=0}$ generated by the nonlinearities of the junction resistance is dissipated in the load $(P_L|_{\omega=0})$ as well as in the junction resistance and series resistance of the nonlinear device $(P_G|_{\omega=0})$

$$\begin{aligned} P|_{\omega=0} &= P_G|_{\omega=0} + P_L|_{\omega=0} \\ &= (R_j + R_s) i|^2_{\omega=0} + (R_L) i|^2_{\omega=0}. \end{aligned} \tag{12}$$

Using (11), the power dissipated in the load can be then rewritten

$$P_L|_{\omega=0} = P_{R_j}|^2_{\omega=\omega_0} \frac{\Re_I^2 R_j^2 R_L}{(R_j + R_s + R_L)^2}. \tag{13}$$

At ω_0, the diode parasitic components, such as the junction capacitance C_j and the series resistance R_s, as well as the reflection losses prevent the input power of the rectifier $P_{\mathrm{ANT}}|_{\omega=\omega_0}$, usually flowing from an antenna, from fully reaching at the junction [110], [113]

$$P_{R_j}|_{\omega=\omega_0} = P_{\mathrm{ANT}}|_{\omega_0} \eta_M \frac{1}{1 + \dfrac{R_s}{R_j}} \times \frac{1}{1 + \dfrac{R_s}{R_j} + \omega^2 C_j^2 R_j R_s} \tag{14}$$

where η_M is the matching efficiency. The rectifier conversion efficiency can be then written using $R_s \ll R_j$ (which is usually the case) and $R_L = R_j$ [optimum load condition, calculated from (13)]

$$\eta_0 = \frac{P_L|_{\omega=0}}{P_{\mathrm{ANT}}|_{\omega=\omega_0}} = \Re_I^2 P_{\mathrm{ANT}}|_{\omega=\omega_0} \eta_M^2 \left(\frac{\sqrt{R_j}}{2 + 2\omega^2 C_j^2 R_j R_s} \right)^2. \tag{15}$$

The efficiency obtained in (15) is compared to the SPICE simulation in Fig. 28. It can be seen that the model describes well the trends at medium power, while its prediction becomes more accurate at lower power, where the efficiency is linearly power dependent. Efficiency described in (15) will be only compressed at higher power, which means that it can be used to compare the different rectifiers described in Section III.

The devices are then reported in Fig. 29 along with the plot of (15) for different input frequencies, all in the case of $\eta_M = 1$. The conversion mechanism can be well identified in the figure and can be described in the following way: the responsivity lifts the efficiency depending on the rectifier nonlinearities while the parasitics tend to diminish it at higher frequency. Therefore, the fundamental parameter for RF-to-dc conversion is the current responsivity, which is the reason why it is chosen as a central metric of the evolution of technology (Fig. 5). The junction resistance, however, has a completely different impact depending on the operating frequency and the junction

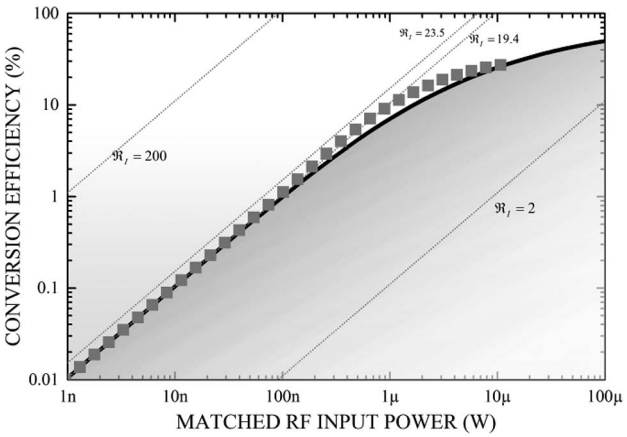

Fig. 28. *Conversion efficiency in a rectifying circuit based on the SMS7630 diode under lossless matched condition. Data obtained from the low power analysis (15) are plotted in a gray short dotted line. A more complicated version of (15) taking into account the deviation from square-law operation Δ and self-biasing V_b is plotted in gray boxes. Those data are compared to a SPICE circuit simulation under the same conditions in black solid line. Frequency is 2.45 GHz and output load is 1 kΩ.*

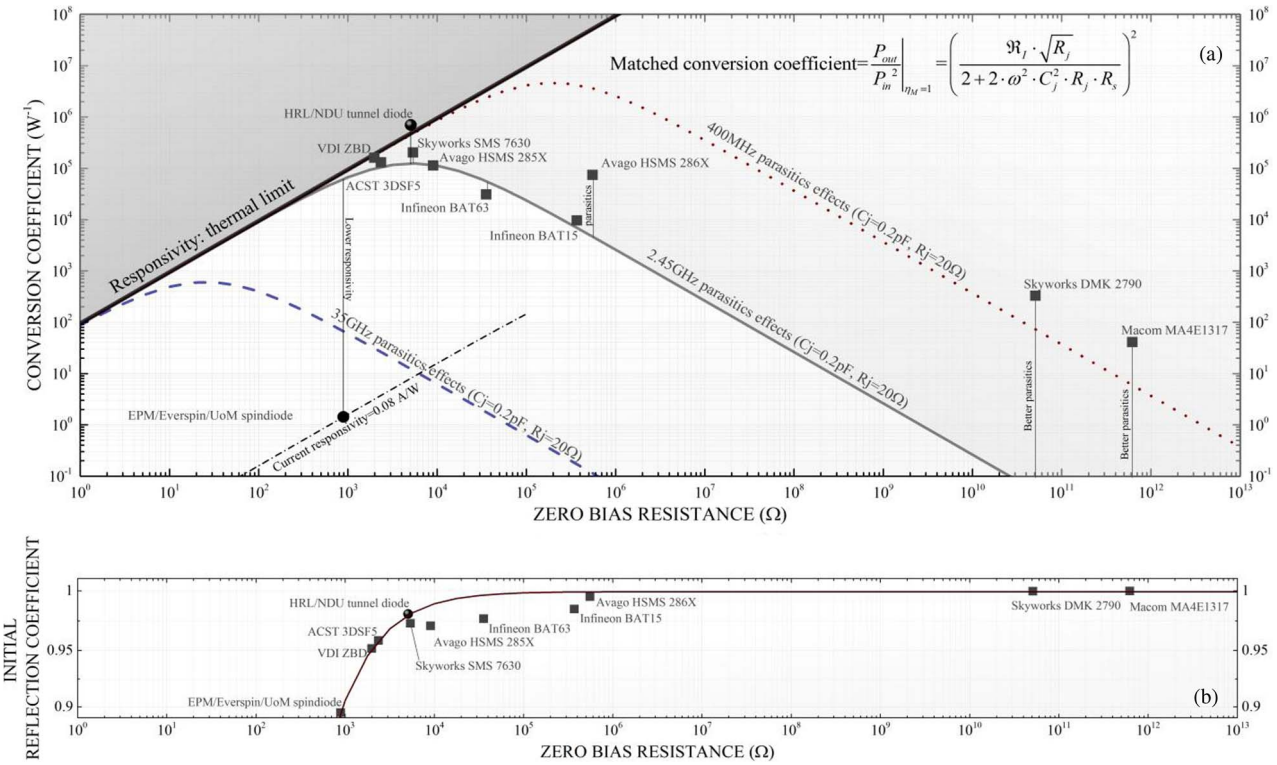

Fig. 29. *(a) Conversion coefficient: ratio efficiency defined in (15) over input power, under lossless matched conditions. The curves are plotted at 0 Hz (bold solid line), at 400 MHz (dotted line), at 2.45 GHz (solid line) and at 35 GHz (dashed line) using typical low barrier diode parasitics value (Rs = 20 Ω and Cj = 0.2 pF). The zero bias resistance stands for the value of the junction resistance. P_{out} and P_{in} stand for the dc power in the load $P_L|_{\omega=0}$ and the power at the input of the rectifier $P_{ANT}|_{\omega=\omega_0}$, respectively. (b) Reflection coefficient calculated from (17) for 2.45 GHz. Data in the solid line are calculated as Rs = 20° and Cj = 0.2 pF.*

capacitance. Therefore, the choice of the junction resistance should be closely dependent on frequency.

There is another factor that the junction resistance will influence: the matching efficiency η_M. Because of the high impedance of the diode, a part of the RF energy received by the antenna might be reflected back. This behavior is quantified by reflection coefficient ρ_0 (see Fig. 27). To avoid this loss, a matching circuit should be used, but this operation can in some cases induce its own losses [115]. It can be understood easily with a simple stage matching case, for which the matching efficiency can be written

$$\eta_M = \frac{1}{1+\dfrac{Q}{Q_c}} \tag{16}$$

where Q is the matching network quality factor and Q_c is the net component quality factor. The matching network consists in a circuit that would affect the propagation with the aim to cancel the reflected wave. This circuit is very similar to a resonator, whose quality factor directly depends on the initial unmatched reflection coefficient $Q = f(\rho_0)$. But the components that are used to build this circuit are not perfect, and their intrinsic losses can affect the matching circuit performances. The net component quality factor is used to describe this nonideality: $Q_c = f(1/R_c)$ with R_c the equivalent parasitic resistance of those components. To maximize the matching efficiency, $Q \ll Q_c$ should be satisfied. Since R_c depends on the circuit technology that is constrained in most cases, the designer would prefer to limit the reflection ρ_0. For the simple case of a 50-Ω antenna [116], it can be written

$$|\rho_0|^2 = \frac{\left(R_j + (R_s - 50)\left(C_j^2 R_j^2 \omega^2 + 1\right)\right)^2 + C_j^2 R_j^4 \omega^2}{\left(R_j + (R_s + 50)\left(C_j^2 R_j^2 \omega^2 + 1\right)\right)^2 + C_j^2 R_j^4 \omega^2}. \tag{17}$$

Data are plotted in Fig. 29. The previous analysis explains well why SMS 7630 is the most successfully used low barrier Schottky diode today for the development of gigahertz-frequency electromagnetic energy-harvesting circuits. This is because it has the right zero bias junction resistance with a limited junction capacitance to operate at low gigahertz range. It has an initial reflection coefficient of 0.97, which is close to the maximum coefficient that is

generally possible to match with a low-loss condition. In the hypothetical case of a negligible junction capacitance, going for a larger junction resistance would mean to result in a higher initial reflection coefficient that could be matched only at the expense of a lower efficiency.

As a conclusion, for a given technology and a junction capacitance, there is an optimum junction resistance for each operating frequency.

V. PERSPECTIVES

The future of rectifier technology promises to be thrilling. The diode landscape as we know it is about to change. The past decades have been monotonous: the Schottky diode has ruled alone. Since the maximum responsivity has already been reached now, no major changes could be expected with the current technology set. However, we are going to witness a situation never encountered before. The chronological chart clearly suggests a disruptive game change observable for the near future. The backward diodes have already surpassed the Schottky diodes, and if the current trend continues, the MIM and spindiode will soon do the same. It is hard to say which one is going to dominate. Nevertheless, the certainty is that the performance of RF energy harvester would fully benefit from this technological competition. The major impact is that it will become possible to harvest and convert low-level energy that is not harvestable today. Let us summarize the main points of each technology to walk us through their strengths and weaknesses.

A. Schottky Diode

Although the Schottky diode had basically reached its maximum responsivity a long time ago, it will certainly be important in the next decades. Its technology is by far the most matured. Processes are well established and reliable, meaning that the device will continue to be available at low cost. Some groups are still working on the development of Schottky devices to obtain lower junction resistance and lower junction capacitance. Those features will be useful for millimeter-wave applications. Unfortunately, they will have very little impact on the RF energy-harvesting development [117], [118].

B. Backward Tunnel (Esaki) Diode

The tunnel diode has never been a commercial success, although rectification mechanisms are very elegant. As a matter of fact, it is the technology of the best rectifier ever built up. Research on the tunnel diode largely benefitted from PN diode technologies, and large-scale production of the "top diode" should be possible in the same foundries. It is expected that responsivity of the tunnel diode will continue to grow slowly. A responsivity of nearly 35 A/W has been predicted in 1967 [119], but this limit is dependent on which semiconductor is used. As has been shown before, the junction capacitance is very low, ensuring that no parasitics will affect the RF performances. This diode is probably the best short-term device that would help RF energy harvested to enhance their low-power conversion.

C. MIM Diode

Simple tunnel junction MIM diodes have never been manufactured or commercialized at a large scale. However, since the device makes use of only metal and insulator material, it is expected that the fabrication cost would be competitive. Intensive work is still necessary to improve and enhance the responsivity. The most challenging task will be to build a barrier that is not fully dependent on thermal activation. Otherwise, the device would not be able to pass through the thermal voltage limitation of common Schottky diodes. In this direction, the double insulator technology carries a much anticipated hope [96].

D. Spindiodes (MTJ)

The MTJ technology using MgO barrier is only ten years old, but it is already manufactured for massive MRAM applications. Although the fabrication process of spindiode is very complex, spindiode can benefit from a large market of MRAM that could guarantee an easy fabrication, eventually at a lower cost. From the understanding of rectification mechanisms, MTJ is clearly favored by the spin-dependent transport, and even if actual responsivity is very low because of a weak nonlinearity with the current spindiode samples available to us, a high responsivity is expected if the spindiode can be engineered to meet the requirements of nonlinearity. In some cases, the spin-torque diode effect could also provide a step further to reach higher performances. As for parasitic limitations, research efforts on interfacial resistance are expected to play a positive role in improving the frequency behavior.

E. Improvement of Efficiency by Using Different Sources

Energy harvesters are used to power various devices, in particular mobile and wireless devices. Generally speaking, there is no reason to limit harvesting to only one electromagnetic RF ambient power if other sources are abundantly available. Other energy can be found in the form of kinetic, chemical, or other electromagnetic sources (heat radiation, sun, etc.). Therefore, the future of energy harvesting could be determined by our ability to make those energies interacting and exchanged in order to improve efficiency. This is a typical hybrid approach, which has found many successful stories today such as hybrid vehicles.

VI. CONCLUSION

The high performance of an RF-to-dc conversion circuit or system depends mostly on the performance of its involved rectifier. In turn, the performance of this rectifier is depending on the magnitude of resistance variation

(nonlinearity) of the device involved. Potential barriers along with thermionic emission have been the first mechanism to be successfully harnessed, and used at a large scale in the Schottky diode. The limitation of a thermionic emission-based rectification, namely the thermal voltage, was reached 50 years ago. Since then, Schottky diode technologies have not evolved much. In the past decades, other technologies have emerged and are now about to challenge the superiority of the decades-old technology. Tunnel diodes, MIM diodes, and MTJ all have the possibility to surpass the Schottky diode, which will in turn open a new avenue for low-power energy harvesting limited today by the thermal voltage restrictions. In addition, those emerging diode technologies will also change the landscape of future electronic circuits and systems as they present many promising and interesting features in the design and development of nonlinear devices such as future low-power transceiver research and innovations. ■

Acknowledgment

The authors would like to thank D. Houssameddine, C. H. P. Lorenz, Y. Gui, M. Chin, P. Fay, J. Gauthier, and C.-M. Hu for fruitful discussions and stimulation. They would also like to thank the reviewers for making many useful suggestions.

REFERENCES

[1] M. A. Toman and B. Jemelkova, "Energy and economic development: An assessment of the state of knowledge," *Energy J.*, vol. 24, pp. 93–112, 2003.

[2] A. Grubler *et al.*, "Energy primer," *Global Energy Assessment-Toward a Sustainable Future*. Cambridge, U.K.: Cambridge Univ. Press, 2012, pp. 99–150.

[3] T. B. Johansson, A. P. Patwardhan, N. Nakićenović, and L. Gomez-Echeverri, *Global Energy Assessment: Toward a Sustainable Future*. Cambridge, U.K.: Cambridge Univ. Press, 2012.

[4] J. M. Gohlke *et al.*, "Estimating the global public health implications of electricity and coal consumption," *Environ. Health Perspectives*, vol. 119, pp. 821–826, 2011.

[5] K. R. Smith and M. Ezzati, "How environmental health risks change with development: The Epidemiologic and environmental risk transitions revisited," *Annu. Rev. Environ. Resources*, vol. 30, pp. 291–333, 2005.

[6] K. R. Smith *et al.*, "Energy and human health," *Annu. Rev. Public Health*, vol. 34, pp. 159–188, 2013.

[7] H. Farhangi, "The path of the smart grid," *IEEE Power Energy Mag.*, vol. 8, no. 1, pp. 18–28, Jan./Feb. 2010.

[8] M. Green, "Thin-film solar cells: Review of materials, technologies, and commercial status," *J. Mater. Sci., Mater. Electron.*, vol. 18, pp. 15–19, 2007.

[9] A. Khaligh, Z. Peng, and Z. Cong, "Kinetic energy harvesting using piezoelectric and electromagnetic technologies—State of the art," *IEEE Trans. Ind. Electron.*, vol. 57, no. 3, pp. 850–860, Mar. 2010.

[10] J. M. Carrasco *et al.*, "Power-electronic systems for the grid integration of renewable energy sources: A survey," *IEEE Trans. Ind. Electron.*, vol. 53, no. 4, pp. 1002–1016, Jun. 2006.

[11] J. J. Thomson, "Carriers of negative electricity," Nobel Lecture, 1906.

[12] K. F. Braun, "Electrical oscillations and wireless telegraphy," Nobel Lecture, December 1909, vol. 11, pp. 226–245.

[13] G. Marconi, "Wireless telegraphic communication," Nobel Lecture, Dec. 1909, vol. 11, pp. 196–222.

[14] M. Planck, "The genesis and present state of development of the quantum theory," Nobel Lecture, 1920, vol. 2, pp. 1–10.

[15] N. Bohr, "The structure of the atom," Nobel Lecture, 1922, vol. 11, p. 1922.

[16] L. De Broglie, "The wave nature of the electron," Nobel Lecture, 1929, vol. 12, pp. 244–256.

[17] W. Heisenberg, "The development of quantum mechanics," in *Scientific Review Papers, Talks, Books*. New York, NY, USA: Springer-Verlag, 1984, pp. 226–237.

[18] I. Langmuir, "Surface chemistry," *Chem. Rev.*, vol. 13, pp. 147–191, 1933.

[19] E. Schrödinger, "The fundamental idea of wave mechanics," *Resonance*, vol. 4, pp. 92–103, 1999.

[20] P. A. Dirac, "Theory of electrons and positrons," Nobel Lecture, 1933, vol. 12, pp. 320–325.

[21] E. Fermi, E. Amaldi, O. D'Agostino, and F. Rasetti, "Artificial radioactivity produced by neutron bombardment," *Proc. Roy. Soc. Lond. A*, vol. 146, pp. 483–500, 1934.

[22] W. Pauli, *Exclusion Principle and Quantum Mechanics*. New York, NY, USA: Springer-Verlag, 1994.

[23] P. W. Bridgman, "General survey of certain results in the field of high-pressure physics," Nobel Lecture, Dec. 1946, vol. 11, p. 1946.

[24] P. Kusch and H. Foley, "The magnetic moment of the electron," *Phys. Rev.*, vol. 74, 1948, 250.

[25] W. H. Brattain, "Surface properties of semiconductors," *Science*, vol. 126, pp. 151–153, 1957.

[26] J. Bardeen, "Research leading to point-contact transistor," *Science*, vol. 126, pp. 105–112, 1957.

[27] L. Néel, "Magnetism and the local molecular field," *Science*, vol. 174, pp. 985–992, 1971.

[28] L. Esaki, "Long journey into tunneling," *Rev. Modern Phys.*, vol. 46, pp. 237–244, 1974.

[29] P. W. Anderson, "Local moments and localized states," *Rev. Modern Phys.*, vol. 50, pp. 191–201, 1978.

[30] N. Mott, "Electrons in glass," *Science*, vol. 201, pp. 871–875, 1978.

[31] J. Van Vleck, "Quantum mechanics—The key to understanding magnetism," *Rev. Modern Phys.*, vol. 50, pp. 181–189, 1978.

[32] Z. I. Alferov, "Nobel Lecture: The double heterostructure concept and its applications in physics, electronics, and technology," *Rev. Modern Phys.*, vol. 73, pp. 767–782, 2001.

[33] H. Kroemer, "Quasi-electric fields and band offsets: Teaching electrons new tricks," Nobel Lecture, Dec. 2000, vol. 8, pp. 449–469.

[34] J. S. C. Kilby, "Turning potential into realities: The invention of the integrated circuit (Nobel lecture)," *Chem. Phys. Chem.*, vol. 2, pp. 482–489, 2001.

[35] A. Fert, "Nobel Lecture: Origin, development, future of spintronics," *Rev. Modern Phys.*, vol. 80, pp. 1517–1530, 2008.

[36] P. A. Grünberg, "From spinwaves to Giant Magnetoresistance (GMR) and beyond," Nobel Lecture, 2007, pp. 92–108.

[37] Z. Popovic and E. N. Grossman, "THz metrology and instrumentation," *IEEE Trans. Terahertz Sci. Technol.*, vol. 1, no. 1, pp. 133–144, Sep. 2011.

[38] C. Ho, S. Slobin, A. Kantak, and S. Asmar, "Solar brightness temperature and corresponding antenna noise temperature at microwave frequencies," Interplanetary Netw. Progr. Rep., 2008, pp. 42–175.

[39] D. J. Vermeulen, "A Popov lightning recorder?—In South Africa!" Proc. IEEE, vol. 88, no. 12, pp. 1972–1975, Dec. 2000.

[40] L. F. Fuller, "The design of Poulsen arc converters for radio telegraphy," *Proc. Inst. Radio Eng.*, vol. 7, pp. 449–497, 1919.

[41] F. Carassa, "On the 80th anniversary of the first transatlantic radio signal," *IEEE Antennas Propag. Soc. Newslett.*, vol. 24, no. 6, pp. 10–19, Dec. 1982.

[42] L. De Forest, "Recent developments in the work of the federal telegraph company," *Proc. Inst. Radio Eng.*, vol. 1, pp. 37–51, 1913.

[43] G. E. Valley and H. Wallman, *Vacuum Tube Amplifiers*. New York, NY, USA: McGraw-Hill, 1948.

[44] H. A. H. Boot and J. T. Randall, "Historical notes on the cavity magnetron," *IEEE Trans. Electron Devices*, vol. ED-23, no. 7, pp. 724–729, Jul. 1976.

[45] D. Varian, "From the inventor and the Pilot Russell and Sigurd Varian," *IEEE Trans. Microw. Theory Tech.*, vol. MTT-32, no. 9, pp. 1248–1263, Sep. 1984.

[46] D. N. McQuiddy, Jr., J. W. Wassel, J. B. LaGrange, and W. R. Wisseman, "Monolithic microwave integrated circuits: An historical perspective," *IEEE Trans. Microw. Theory Tech.*, vol. MTT-32, no. 9, pp. 997–1008, Sep. 1984.

[47] D. Mavrakis, "Small Cell Market Status—December 2012," London, U.K., 2012.

[48] D. Watkins, *Embedded WLAN (Wi-Fi) CE Devices: Global Market Forecast*. Boston, MA, USA: Strategy Analytics, 2014.

[49] B. Sanou, "ICT Facts and Figures," International Telecommunication Union, Geneva, Switzerland, 2013.

[50] "RF spectral survey in London: Measurements at the Mile End metro station," 2012. [Online]. Available: http://www.londonrfsurvey.org/#

[51] J. G. Koomey, S. Berard, M. Sanchez, and H. Wong, "Implications of historical trends in the electrical efficiency of computing," *IEEE Ann. History Comput.*, vol. 33, no. 3, pp. 46–54, Mar. 2011.

[52] S. Hemour *et al.*, "Towards low-power high-efficiency rf and microwave energy harvesting," *IEEE Trans. Microw. Theory Tech.*, vol. 62, no. 4, pt. 2, pp. 965–976, Apr. 2014.

[53] F. Braun, "Ueber die Stromleitung durch Schwefelmetalle," *Annalen der Physik*, vol. 229, pp. 556–563, 1875.

[54] A. Schuster, "XXXVI. On unilateral conductivity," *London, Edinburgh, Dublin Philosoph. Mag. J. Sci.*, vol. 48, pp. 251–258, 1874.

[55] J. S. Belrose, "Reginald Aubrey Fessenden and the birth of wireless telephony," *IEEE Antennas Propag. Mag.*, vol. 44, no. 2, pp. 38–47, Apr. 2002.

[56] H. W. Secor, "Radio detector development," *Electr. Exp.*, vol. 4, no. 9, 1917. [Online]. Available: http://earlyradiohistory.us/1917de.htm

[57] P. S. Carter and H. H. Beverage, "Early history of the antennas and propagation field until the end of World War I, Part I—Antennas," *Proc. IRE*, vol. 50, pp. 679–682, 1962.

[58] J. M. Dilhac, "Edouard Branly, the Coherer, the Branly effect," *IEEE Commun. Mag.*, vol. 47, no. 9, pp. 20–26, Sep. 2009.

[59] B. van Loon, "Radar 101: Celebrating 101 years of development," *Proc. IEEE*, vol. 93, no. 4, pp. 844–846, Apr. 2005.

[60] M. Guarnieri, "The age of vacuum tubes: Early devices and the rise of radio communications," *IEEE Ind. Electron. Mag.*, vol. 6, no. 1, pp. 41–43, Mar. 2012.

[61] H. F. Dylla and S. T. Corneliussen, "John Ambrose Fleming and the beginning of electronics," *J. Vacuum Sci. Technol. A, Vacuum Surfaces Films*, vol. 23, pp. 1244–1251, 2005.

[62] S. Maas, "Armstrong and the Superheterodyne: A historical look at the mixer," *IEEE Microw. Mag.*, vol. 14, no. 6, pp. 34–39, Sep./Oct. 2013.

[63] J. E. Brittain, "Electrical engineering hall of fame: Lee de Forest," *Proc. IEEE*, vol. 93, no. 1, pp. 198–202, Jan. 2005.

[64] A. Banti, "La telegrafia senza fili e la R. Marina Italiana," *L'Elettricista, Series II*, pp. 113–119, 1902, See the English translation in "The Castelli coherer," *Electrician*, Jun. 27, 1902.

[65] P. K. Bondyopadhyay, "Sir J.C. Bose diode detector received Marconi's first transatlantic wireless signal of December 1901 (the 'Italian Navy Coherer' Scandal Revisited)," *Proc. IEEE*, vol. 86, no. 1, pp. 259–285, Jan. 1998.

[66] A. I. Khan, "Pre-1900 semiconductor research and semiconductor device applications," in *Proc. IEEE Conf. History Electron.*, 2004, pp. 1–21. [Online]. Available: http://www.ieeeghn.org/wiki/images/0/09/Khan.pdf

[67] D. P. C. Thackeray, "Communications: When tubes beat crystals: Early radio detectors: Although crystals were superior, tubes won out—Until the solid-state revolution reversed tradition with a different kind of 'crystal' detector," *IEEE Spectrum*, vol. 20, no. 3, pp. 64–69, Mar. 1983.

[68] G. W. Pierce, "Crystal rectifiers for electric currents and electric oscillations. II. Carborundum, Molybdenite, Anatase, Brookite," *Proc. Amer. Acad. Arts Sci.*, vol. 44, pp. 317–349, 1909.

[69] P. R. Coursey, "Some characteristic curves and sensitiveness tests of crystal and other detectors," *Proc. Phys. Soc. Lond.*, vol. 26, 1913, DOI: 10.1088/1478-7814/26/1/310.

[70] L. W. Austin, "The high resistance contact thermo-electric detector for electrical waves," *Phys. Rev. I*, vol. 24, pp. 508–510, 1907.

[71] H. C. W. Torrey, C. Austin, and S. A. Goudsmit, *Crystal Rectifiers*. New York, NY, USA: McGraw-Hill, 1948.

[72] J. F. Corrigan, *The "P.W." Crystal Experimenter's Handbook: Information You Cannot Do Without*. London, U.K.: Amalgamated Press, 1922, 1925.

[73] R. Ohl, *Interview of Russel Ohl by Lillian H Hoddeson*, L. H. Hoddeson, Ed. College Park, MD, USA: AIP, 1976.

[74] R. S. Ohl, "Properties of ionic bombarded silicon," *Bell Syst. Tech. J.*, vol. 31, pp. 104–121, 1952.

[75] J. H. Scaff and R. S. Ohl, "Development of silicon crystal rectifiers for microwave radar receivers," *Bell Syst. Tech. J.*, vol. 26, pp. 1–30, 1947.

[76] G. L. Pearson and W. H. Brattain, "History of semiconductor research," *Proc. IRE*, vol. 43, pp. 1794–1806, 1955.

[77] D. Kahng and L. A. D'Asaro, "Gold-epitaxial silicon high-frequency diodes," *Bell Syst. Tech. J.*, vol. 43, pp. 225–232, 1964.

[78] D. Kahng and M. P. Lepselter, "Planar epitaxial silicon Schottky barrier diodes," *Bell Syst. Tech. J.*, vol. 44, pp. 1525–1528, 1965.

[79] M. P. Lepselter and S. M. Sze, "Silicon Schottky barrier diode with near-ideal I–V characteristics," *Bell Syst. Tech. J.*, vol. 47, pp. 195–208, 1968.

[80] H. V. Shurmer, "Recent developments in silicon radar crystals," *Proc. Inst. Electr. Eng.*, vol. 111, pp. 257–263, 1964.

[81] M/A-COM Technol. Solutions Inc., "GaAs flip chip Schottky barrier diodes," Lowell, MA, USA, MA4E1317 datasheet, 2001.

[82] Skyworks Inc., "Surface mount mixer and detector Schottky diodes," Woburn, MA, USA, SMS 7630 datasheet, 2000.

[83] J. N. Schulman *et al.*, "Quantum tunneling Sb-heterostructure millimeter-wave diodes," in *Tech. Dig. Int. Electron Devices Meeting*, 2001, pp. 35.1.1–35.1.3.

[84] N. Su, R. Rajavel, P. Deelman, J. N. Schulman, and P. Fay, "Sb-heterostructure millimeter-wave detectors with reduced capacitance and noise equivalent power," *IEEE Electron Device Lett.*, vol. 29, no. 6, pp. 536–539, Jun. 2008.

[85] Z. Ze, R. Rajavel, P. Deelman, and P. Fay, "Sub-micron area heterojunction backward diode millimeter-wave detectors with 0.18 pW/Hz∧(1/2) noise equivalent power," *IEEE Microw. Wireless Compon. Lett.*, vol. 21, no. 5, pp. 267–269, May 2011.

[86] L. Esaki, "New phenomenon in narrow germanium p-n junctions," *Phys. Rev.*, vol. 109, pp. 603–604, 1958.

[87] L. Nordheim, "Zur Theorie der thermischen Emission und der Reflexion von Elektronen an Metallen," *Zeitschrift für Physik*, vol. 46, pp. 833–855, 1928.

[88] E. Merzbacher, "The early history of quantum tunneling," *Phys. Today*, vol. 55, pp. 44–50, 2002.

[89] J. G. Simmons, "Potential barriers and emission—Limited current flow between closely spaced parallel metal electrodes," *J. Appl. Phys.*, vol. 35, pp. 2472–2481, 1964.

[90] E. Sakuma and K. Evenson, "Characteristics of tungsten-nickel point contact diodes used as laser harmonic-generator mixers," *IEEE J. Quantum Electron.*, vol. QE-10, no. 8, pp. 599–603, Aug. 1974.

[91] D. A. Jennings, F. R. Petersen, and K. M. Evenson, "Extension of absolute frequency measurements to 148 THz: Frequencies of the 2.0- and 3.5-μm Xe laser," *Appl. Phys. Lett.*, vol. 26, pp. 510–511, 1975.

[92] W. F. Brinkman, R. C. Dynes, and J. M. Rowell, "Tunneling conductance of asymmetrical barriers," *J. Appl. Phys.*, vol. 41, pp. 1915–1921, 1970.

[93] J.-I. Shirakashi, K. Matsumoto, N. Miura, and M. Konagai, "Nb/Nb oxide-based planar-type metal/insulator/metal (MIM) diodes fabricated by atomic force microscope (AFM) nano-oxidation process," *Jpn. J. Appl. Phys*, vol. 36, no. 8B, pt. 2, pp. L1120–L1122, 1997, DOI: 10.1143/JJAP.36.L1120.

[94] S. Rockwell *et al.*, "Characterization and modeling of metal/double-insulator/metal diodes for millimeter wave wireless receiver applications," in *Proc. IEEE Radio Frequency Integr. Circuits Symp.*, 2007, pp. 171–174.

[95] K. Choi *et al.*, "Geometry enhanced asymmetric rectifying tunneling diodes," *J. Vacuum Sci. Technol. B*, vol. 28, pp. C6O50–C6O55, 2010.

[96] S. Grover and G. Moddel, "Engineering the current-voltage characteristics of metal-insulator-metal diodes using double-insulator tunnel barriers," *Solid-State Electron.*, vol. 67, pp. 94–99, 2012.

[97] M. L. Chin *et al.*, "Planar metal-insulator-metal diodes based on the Nb/Nb2O5/X material system," *J. Vacuum Sci. Technol. B, Microelectron. Nanometer Structures*, vol. 31, pp. 051204-1–051204-8, 2013.

[98] N. F. Mott, "The electrical conductivity of transition metals," *Proc. Roy. Soc. Lond. A, Math. Phys. Sci.*, vol. 153, pp. 699–717, Feb. 1936.

[99] C. Chappert, A. Fert, and F. N. Van Dau, "The emergence of spin electronics in data storage," *Nature Mater.*, vol. 6, pp. 813–823, 2007.

[100] M. Julliere, "Tunneling between ferromagnetic films," *Phys. Lett. A*, vol. 54, pp. 225–226, 1975.

[101] S. Hemour *et al.*, "Spintronics-based devices for microwave power harvesting," in *IEEE MTT-S Int. Microw. Symp. Dig.*, 2012, DOI: 10.1109/MWSYM.2012.6259629.

[102] J. S. Moodera, L. R. Kinder, T. M. Wong, and R. Meservey, "Large magnetoresistance at room temperature in ferromagnetic thin film tunnel junctions," *Phys. Rev. Lett.*, vol. 74, pp. 3273–3276, 1995.

[103] S. Yuasa, T. Nagahama, A. Fukushima, Y. Suzuki, and K. Ando, "Giant room-temperature magnetoresistance in single-crystal Fe/MgO/Fe magnetic tunnel junctions," *Nature Mater.*, vol. 3, pp. 868–871, 2004.

[104] J. Åkerman, "Toward a universal memory," *Science*, vol. 308, pp. 508–510, Apr. 22, 2005.

[105] A. A. Tulapurkar *et al.*, "Spin-torque diode effect in magnetic tunnel junctions," *Nature*, vol. 438, pp. 339–342, 2005.

[106] S. Zhang, "Spin-dependent surface screening in ferromagnets and magnetic tunnel junctions," *Phys. Rev. Lett.*, vol. 83, pp. 640–643, 1999.

[107] G. Landry, Y. Dong, J. Du, X. Xiang, and J. Q. Xiao, "Interfacial capacitance effects in magnetic tunneling junctions," *Appl. Phys. Lett.*, vol. 78, pp. 501–503, 2001.

[108] S. Miwa *et al.*, "Highly sensitive nanoscale spin-torque diode," *Nature Mater.*, vol. 13, pp. 50–56, 2014.

[109] W. C. Brown, "Free-space microwave power transmission study, combined phase III and final report, Raytheon Rep. PT-4601, Sep. 1975, Nasa Contract NAS-8-253741975.

[110] T. W. Yoo and C. Kai, "Theoretical and experimental development of 10 and 35 GHz rectennas," *IEEE Trans. Microw. Theory Tech.*, vol. 40, no. 6, pp. 1259–1266, Jun. 1992.

[111] G. Jiapin, Z. Hongxian, and Z. Xinen, "Theoretical analysis of RF-DC conversion efficiency for class-F rectifiers," *IEEE Trans. Microw. Theory Tech.*, vol. 62, no. 4, pt. 2, pp. 977–985, Apr. 2014.

[112] M. Roberg, T. Reveyrand, I. Ramos, E. A. Falkenstein, and Z. Popovic, "High-efficiency harmonically terminated diode and transistor rectifiers," *IEEE Trans. Microw. Theory Tech.*, vol. 60, no. 12, pt. 2, pp. 4043–4052, Dec. 2012.

[113] I. J. Bahl and P. Bhartia, *Microwave Solid State Circuit Design*. New York, NY, USA: Wiley, 1988.

[114] A. M. Cowley and H. O. Sorensen, "Quantitative comparison of solid-state microwave detectors," *IEEE Trans. Microw. Theory Tech.*, vol. MTT-14, no. 12, pp. 588–602, Dec. 1966.

[115] A. M. Niknejad, *Electromagnetics for High-Speed Analog and Digital Communication Circuits*. Cambridge, U.K.: Cambridge Univ. Press, 2007.

[116] D. M. Pozar, *Microwave Engineering*. New York, NY, USA: Wiley, 2009.

[117] E. R. Brown, A. C. Young, J. Zimmerman, H. Kazemi, and A. C. Gossard, "Advances in Schottky rectifier performance," *IEEE Microw. Mag.*, vol. 8, no. 3, pp. 54–59, Jun. 2007.

[118] M. Hoefle *et al.*, "Highly responsive planar millimeter wave zero-bias Schottky detector with impedance matched folded dipole antenna," in *IEEE MTT-S Int. Microw. Symp. Dig.*, 2013, DOI: 10.1109/MWSYM.2013.6697580.

[119] J. Karlovský, "The curvature coefficient of germanium tunnel and backward diodes," *Solid-State Electron.*, vol. 10, pp. 1109–1111, 1967.

ABOUT THE AUTHORS

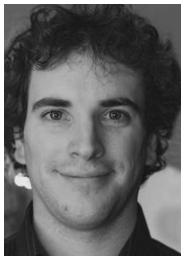

Simon Hemour (Member, IEEE) received the B.S. degree in electrical engineering from the University of Grenoble, Grenoble, France, in 2004 and the M.S. and Ph.D. degrees in optics, optoelectronics, and microwave engineering from the Grenoble Institute of Technology, Grenoble, France, in 2006 and 2010, respectively.

In 2003, he was with the European Organization for Nuclear Research (CERN), Geneva, Switzerland, as a part of the Instrumentation Department, where he was involved with the ATLAS experiment on the Large Haddon Collided (LHC). From 2006 to 2007, he was a Research Assistant with the Pidstryhach Institute of Applied Problems of Mechanics and Mathematics (IAPMM), National Academy of Science of Ukraine (NASU), Lviv, Ukraine. In 2007, he joined the IMEP–LAHC MINATEC Laboratory, Grenoble, France. Since 2011, he has been with the Poly-Grames Research Center, Ecole Polytechnique de Montréal, Montréal, QC, Canada, leading the wireless power transmission and harvesting group. He is currently a Research Associate. His research interest include wireless power transfer and energy harvesting, ferrite-based RF circuits, nonlinear devices, innovative RF measurements, RF interferometry, low-power microwave, and millimeter-wave conversion circuits.

Dr. Hemour is a member of the IEEE MTT-26 "Wireless Energy Transfer and Conversion" Technical Committee.

Ke Wu (Fellow, IEEE) received the B.Sc. degree (with distinction) in radio engineering from Nanjing Institute of Technology (now Southeast University), Nanjing, Jiangsu, China, in 1982, the D.E.A. degree in optics, optoelectronics, and microwave engineering (with distinction) from the Institut National Polytechnique de Grenoble (INPG), Grenoble, France, in 1984, and the Ph.D. degree in optics, optoelectronics, and microwave engineering (with distinction) from the University of Grenoble, Grenoble, France, in 1987.

He is the Professor of Electrical Engineering and Tier-I Canada Research Chair in RF and millimeter-wave engineering at the Ecole Polytechnique, University of Montréal, Montréal, QC, Canada. He has been the Director of the Poly-Grames Research Center. He was the founding Director of the Center for Radiofrequency Electronics Research of Quebec (Regroupement stratégique of FRQNT). He has also held guest, visiting, and honorary professorship at many universities around the world. He authored or coauthored over 990 refereed papers, and a number of books/book chapters and filed more than 30 patents. His current research interests involve substrate integrated circuits (SICs), antenna arrays, advanced computer-aided design (CAD) and modeling techniques, wireless power transmission and harvesting, and development of low-cost RF and millimeter-wave transceivers and sensors for wireless systems and biomedical applications. He is also interested in the modeling and design of microwave and terahertz photonic circuits and systems.

Dr. Wu is a member of the Electromagnetics Academy, the Sigma Xi Honorary Society, and the International Union of Radio Science (URSI). He has held key positions in and has served on various panels and international committees, including the chair of technical program committees, international steering committees, and international conferences/symposia. In particular, he was the General Chair of the 2012 IEEE Microwave Theory and Techniques Society (MTT-S) International Microwave Symposium. He has served on the editorial/review boards of many technical journals, transactions, proceedings, and letters as well as scientific encyclopedia including editors and guest editors. He is currently the Chair of the joint IEEE chapters of MTTS/APS/LEOS in Montréal, QC, Canada. He is an elected IEEE MTT-S AdCom member for 2006–2015 and served as Chair of the IEEE MTT-S Transnational Committee, Member, and Geographic Activities (MGA) Committee and Technical Coordinating Committee (TCC) among many other AdCom functions. He is the inaugural three-year representative of North America as Member of the European Microwave Association (EuMA) General Assembly from January 2014 to December 2016. He was the recipient of many awards and prizes, including the first IEEE MTT-S Outstanding Young Engineer Award, the 2004 Fessenden Medal of the IEEE Canada, the 2009 Thomas W. Eadie Medal of the Royal Society of Canada, the Queen Elizabeth II Diamond Jubilee Medal in 2013, the 2013 FCCP Education Foundation Award of Merit, and the 2014 IEEE MTT-S Microwave Application Award. He is a Fellow of the Canadian Academy of Engineering (CAE) and a Fellow of the Royal Society of Canada (The Canadian Academy of the Sciences and Humanities). He was an IEEE MTT-S Distinguished Microwave Lecturer from January 2009 to December 2011.